

PL-TR-96-2159

**REGIONAL ATTENUATION AT GSETT-3
STATIONS AND THE TRANSPORTABILITY
OF THE Lg/P DISCRIMINANT**

**Richard D. Jenkins
Aaron A. Velasco
Donna J. Williams
Thomas J. Sereno**

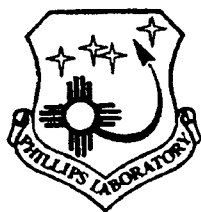
**Science Applications International Corporation
10260 Campus Point Drive
San Diego, CA 92121-1578**

15 July 1996

Scientific Report No. 1

19961104 104

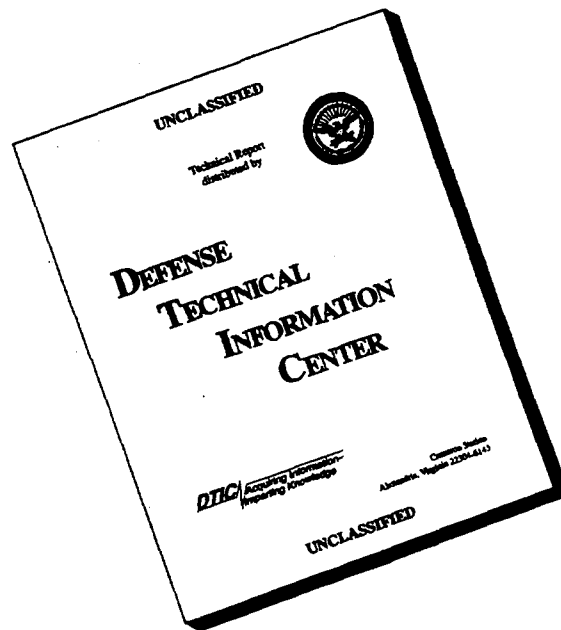
Approved for public release; distribution unlimited



**PHILLIPS LABORATORY
Directorate of Geophysics
AIR FORCE MATERIEL COMMAND
HANSCOM AFB, MA 01731-3010**

DISC QUALITY CONTROL

DISCLAIMER NOTICE




THIS DOCUMENT IS BEST QUALITY AVAILABLE. THE COPY FURNISHED TO DTIC CONTAINED A SIGNIFICANT NUMBER OF PAGES WHICH DO NOT REPRODUCE LEGIBLY.

SPONSORED BY
Department of Energy
Office of Non-Proliferation and National Security

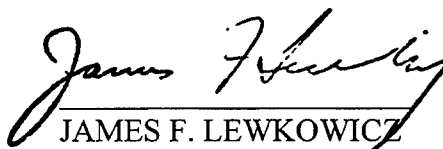
MONITORED BY
Phillips Laboratory
CONTRACT No. F19628-C-0097

The views and conclusions contained in this document are those of the authors and should not be interpreted as representing the official policies, either express or implied, of the Air Force or U.S. Government.

This technical report has been reviewed and is approved for publication.



DELAINE REITER
Contract Manager
Earth Sciences Division



JAMES F. LEWKOWICZ
Director
Earth Sciences Division

This report has been reviewed by the ESD Public Affairs Office (PA) and is releasable to the National Technical Information Service (NTIS).

Qualified requestors may obtain copies from the Defense Technical Information Center. All others should apply to the National Technical Information Service.

If your address has changed, or you wish to be removed from the mailing list, or if the addressee is no longer employed by your organization, please notify PL/IM, 29 Randolph Road, Hanscom AFB, MA 01731-3010. This will assist us in maintaining a current mailing list.

Do not return copies of this report unless contractual obligations or notices on a specific document requires that it be returned.

REPORT DOCUMENTATION PAGE			Form Approved OMB No. 0704-0188	
<small>Public reporting burden for this collection of information is estimated to average 1 hour per response, including the time for reviewing instructions, searching existing data sources, gathering and maintaining the data needed, and completing and reviewing the collection of information. Send comments regarding this burden estimate or any other aspect of this collection of information, including suggestions for reducing this burden, to Washington Headquarters Services, Directorate for Information Operations and Reports, 1215 Jefferson Davis Highway, Suite 1204, Arlington, VA 22202-4302, and to the Office of Management and Budget, Paperwork Reduction Project (0704-0188), Washington, DC 20503.</small>				
1. AGENCY USE ONLY (Leave blank)	2. REPORT DATE July 15, 1996	3. REPORT TYPE AND DATES COVERED Scientific No. 1		
4. TITLE AND SUBTITLE Regional Attenuation at GSETT-3 Stations and the Transportability of the Lg/P Discriminant		5. FUNDING NUMBERS Contract: F19628-95-C-0097 PE69120G PRDENN TA GM WU AO		
6. AUTHOR(S) Richard D. Jenkins, Aaraon A. Velasco, Donna J. Williams, and Thomas J. Sereno, Jr.				
7. PERFORMING ORGANIZATION NAME(S) AND ADDRESS(ES) Science Applications International Corporation 10260 Campus Pt. Drive San Diego CA 92121-1578		8. PERFORMING ORGANIZATION REPORT NUMBER SAIC-96/1137		
9. SPONSORING / MONITORING AGENCY NAME(S) AND ADDRESS(ES) Phillips Laboratory 29 Randolph Road Hanscom AFB, MA 01731-3010 Contract Manager: Delaine Reiter/GPE		10. SPONSORING / MONITORING AGENCY REPORT NUMBER PL-TR-96-2159		
11. SUPPLEMENTARY NOTES				
12a. DISTRIBUTION / AVAILABILITY STATEMENT Approved for public release, distribution unlimited			12b. DISTRIBUTION CODE	
13. ABSTRACT (Maximum 200 words) Recent studies have shown that the high-frequency Lg/P ratio can be an effective discriminant at regional distances. However, this ratio must be recalibrated for each new source region. We are developing regional wave attenuation models for up to 10 subnetworks of the International Data Center (IDC) primary network, and will use them to evaluate the transportability of the Lg/P discriminant to uncalibrated regions. We are measuring amplitudes of regional phases in the time and frequency domain, and using our new software program, AmpInv, to invert for source and attenuation models. During the first year of this two-year project we developed all software needed for this study, investigated alternative amplitude measures, and compiled a data set for an Australian subnetwork. During the second year we will compile the data sets for the other IDC subnetworks, estimate regional wave attenuation using AmpInv, and evaluate the accuracy and transportability of the Lg/P discriminant. We will also obtain "ground-truth" identification for as many of the events as possible, and we will use knowledge of the local natural and industrial seismicity when this information is not available.				
14. SUBJECT TERMS Keywords: Discrimination, Frequency-Dependent Attenuation, Regional Seismicity, Lg/P Ratios, Transportability, Regionalization, Software Development			15. NUMBER OF PAGES 42	
			16. PRICE CODE	
17. SECURITY CLASSIFICATION OF REPORT Unclassified	18. SECURITY CLASSIFICATION OF THIS PAGE Unclassified	19. SECURITY CLASSIFICATION OF ABSTRACT Unclassified	20. LIMITATION OF ABSTRACT Unlimited	

Table of Contents

1.	Introduction.....	1
1.1	Objectives.....	1
1.2	Background	1
1.3	Current Status	1
1.4	Outline of Report.....	2
2.	Data Sets	3
2.1	Station Selection.....	3
2.1.1	Subnetworks.....	3
2.1.2	Tectonic Regionalization	3
2.1.3	Availability of Regional Phases.....	7
2.2	Event Selection.....	8
2.2.1	Attenuation Models.....	8
2.2.1.1	Supplemental Bulletins	9
2.2.2	Lg/P Discriminant.....	13
3.	Attenuation Models	18
3.1	Amplitude Measurements	18
3.2	Inversion Method and Software	19
4.	Summary and Future Work	24
	References	25
	Appendix A: IDC Primary Station Areas	28

1. Introduction

1.1 Objectives

Results from previous empirical studies indicate the high-frequency Lg/P ratio is one of the most promising discriminants at regional distances. However, many of these studies are based on co-located earthquakes and explosions in limited geographic regions, and their results must be recalibrated for each new source region. Our objective is to develop and apply distance corrections for up to 10 stations in the International Data Center (IDC) primary network so that we can evaluate the transportability of the Lg/P discriminant to uncalibrated regions. We will also determine the sensitivity of the Lg/P discriminant to the accuracy of the attenuation models, and attempt to generalize the discriminant by geologic and tectonic regionalization.

1.2 Background

Several early studies propose the use of Lg/P ratios as a regional event discriminant for earthquakes and nuclear explosions [e.g., Willis *et al.*, 1963; Blandford, 1981; Gupta and Burnetti, 1981; Nuttli, 1981; Pomeroy *et al.*, 1982; Murphy and Bennett, 1982; Bennett and Murphy, 1986; Taylor *et al.*, 1989]. These studies found that Lg/P discriminants provide some separation between nuclear explosions and earthquakes, but that there is significant overlap between the two populations. More recent studies have exploited higher frequencies to improve the Lg/P discriminant and have extended the application to include industrial chemical explosions. For example, high-frequency (2-16 Hz) Lg/P ratios have shown to be successful in discriminating between earthquakes and mining explosions in northern and central Europe [e.g., Baumgardt and Young, 1990; Dysart and Pulli, 1990; Baumgardt *et al.*, 1992; Wuster, 1993], and earthquakes and underground nuclear explosions in Eurasia [e.g., Bennett *et al.*, 1989; Chan *et al.*, 1990; Bennett *et al.*, 1992]. The practice of mining can also induce stress-release events such as rockbursts. Often these stress-release events are much larger than the actual mining explosions. Bennett *et al.* [1993] show that stress-release events in central Europe and South Africa have similar Lg/P ratios (> 1.0) to earthquakes across broad frequency bands, and these are higher than the ratios for underground nuclear explosions (< 1.0) at frequencies above 2 Hz. Most of these studies use co-located explosions and earthquakes to minimize propagation effects. A major concern expressed in the recent research is that propagation characteristics may have a significant affect on the Lg/P discriminant, and that transportability may be problematic [e.g., Lynnes and Baumstark, 1991; Bennett *et al.*, 1992].

1.3 Current Status

This report describes our progress in the first year of this two-year effort. We worked on compiling data sets and developing software for generating attenuation models and evaluating the Lg/P discriminant. We modified existing software to measure frequency-

dependent amplitudes, and we are developing new software to invert these amplitudes for source and attenuation parameters.

1.4 Outline of Report

After this brief introduction, this report is divided into three main sections. Section 2 describes the data sets needed for this project and how they were obtained. Section 3 describes progress on our attenuation study which includes investigating alternative amplitude measurements and inverting them for source and attenuation parameters. We have not yet started the discrimination study. Section 4 summarizes our progress and describes our plans for the second year of this project.

2. Data Sets

This section describes the data sets that we are collecting to support our attenuation and discrimination studies. Our primary data source is the Group of Scientific Experts Third Technical Test (called GSETT-3) which is being conducted at the Prototype International Data Center (PIDC) in Arlington, Virginia (for an overview of GSETT-3, see *Kerr* [1993]). The time period of GSETT-3 is from January 1, 1995 to the present. However, we limit this report to include data prior to June 1, 1996. Future reports will include more recent data.

2.1 Station Selection

The IDC is currently receiving data from 46 primary stations and 87 auxiliary stations. As shown in Figure 1, the primary stations are distributed globally. The data from the primary network are sent continuously to the IDC where they are processed and analyzed. Auxiliary stations expand the global coverage of the primary network (Figure 2), but these stations are used only when data are requested to improve the location solutions for events defined by the primary network. We select stations from the IDC primary and auxiliary networks to include in our study based on the ability to form subnetworks of primary and auxiliary stations that are in close proximity (so that events recorded by multiple stations at regional distance are available for the attenuation study), tectonic regionalization, and the availability of regional phases in the IDC Reviewed Event Bulletin, or REB.

2.1.1 Subnetworks

Most primary stations have other primary and auxiliary stations in close proximity. We give preference to these stations because events recorded at multiple stations improve the resolution of the attenuation models. For this reason, we group stations into subnetworks if they are within 40° of each other (we use 20° as the largest distance possible for a regional event). Thus, we define a subnetwork to be comprised of both primary and auxiliary stations. Some IDC primary and auxiliary stations may not be included because they did not have a sufficient number of regional phases (see Section 2.1.3).

2.1.2 Tectonic Regionalization

Eight tectonic regions based on a 2° by 2° grid are defined by *O. Gudmundsson* of the Australian National University [personal communication]. His regionalization is shown in Figure 3. The regions are: Young Ocean (< 25 Ma), Intermediate Ocean (25-100 Ma), Old Ocean (> 100 Ma), Tectonic, Cenozoic Continental, Paleozoic and Mesozoic (150-800 Ma), Proterozoic (800-1700 Ma), and Archean (> 1700 Ma). The Young Ocean, Intermediate Ocean, and Old Ocean categories represent the age of the ocean floor. The Tectonic category represents young and tectonically-active regions. The Cenozoic Continental, Paleozoic and Mesozoic, Proterozoic, and Archean represent young to old relatively stable continental environments. Figure 3 shows the distribution of IDC primary stations in the various geologic and tectonic environments. Note that some station locations fall on the boundary of two adjacent environments. This must be considered when compiling networks that represent different tectonic regions. For the purposes of this study, we combine Cenozoic Continental, Paleozoic and Mesozoic, Proterozoic, and

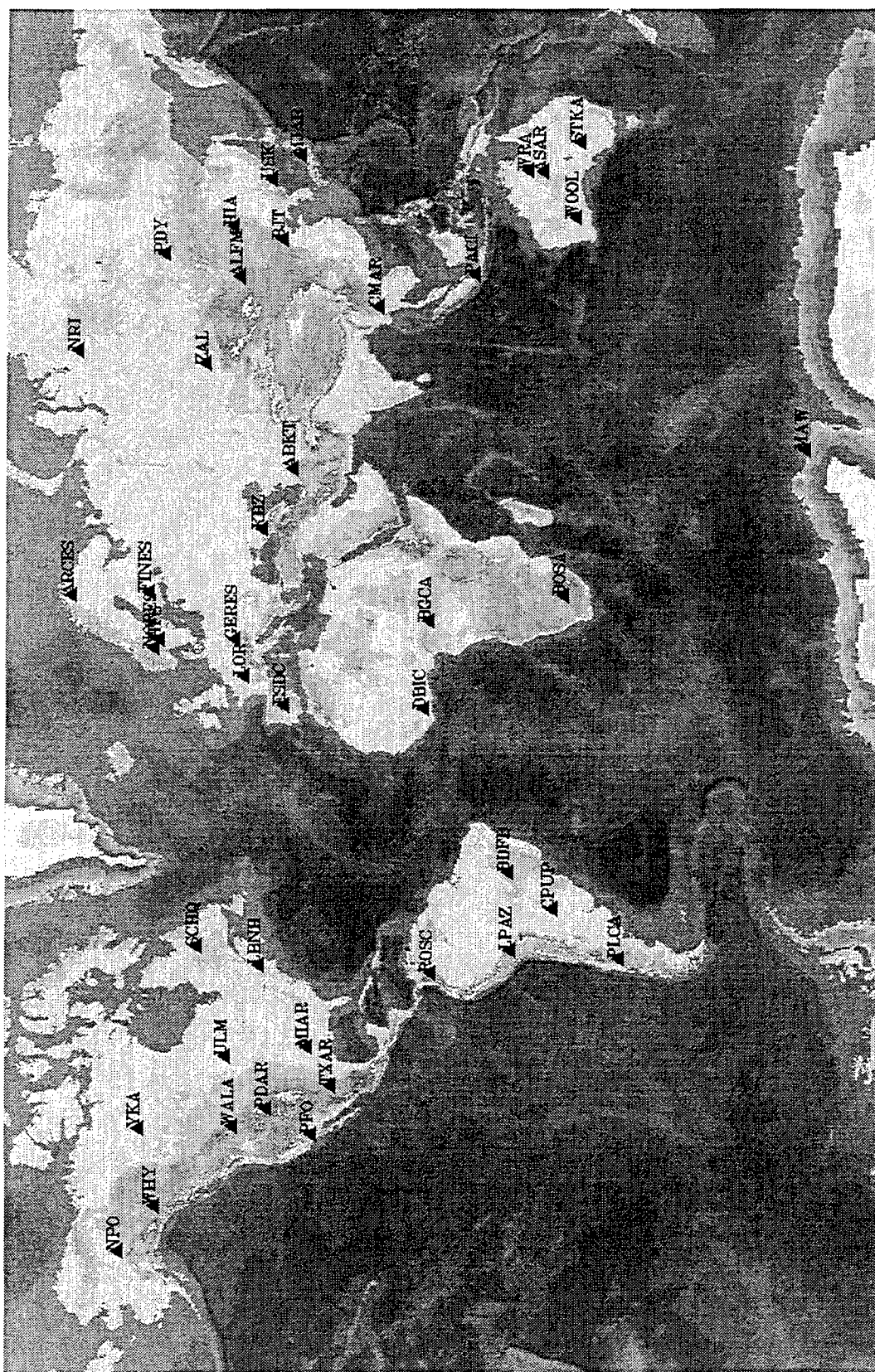
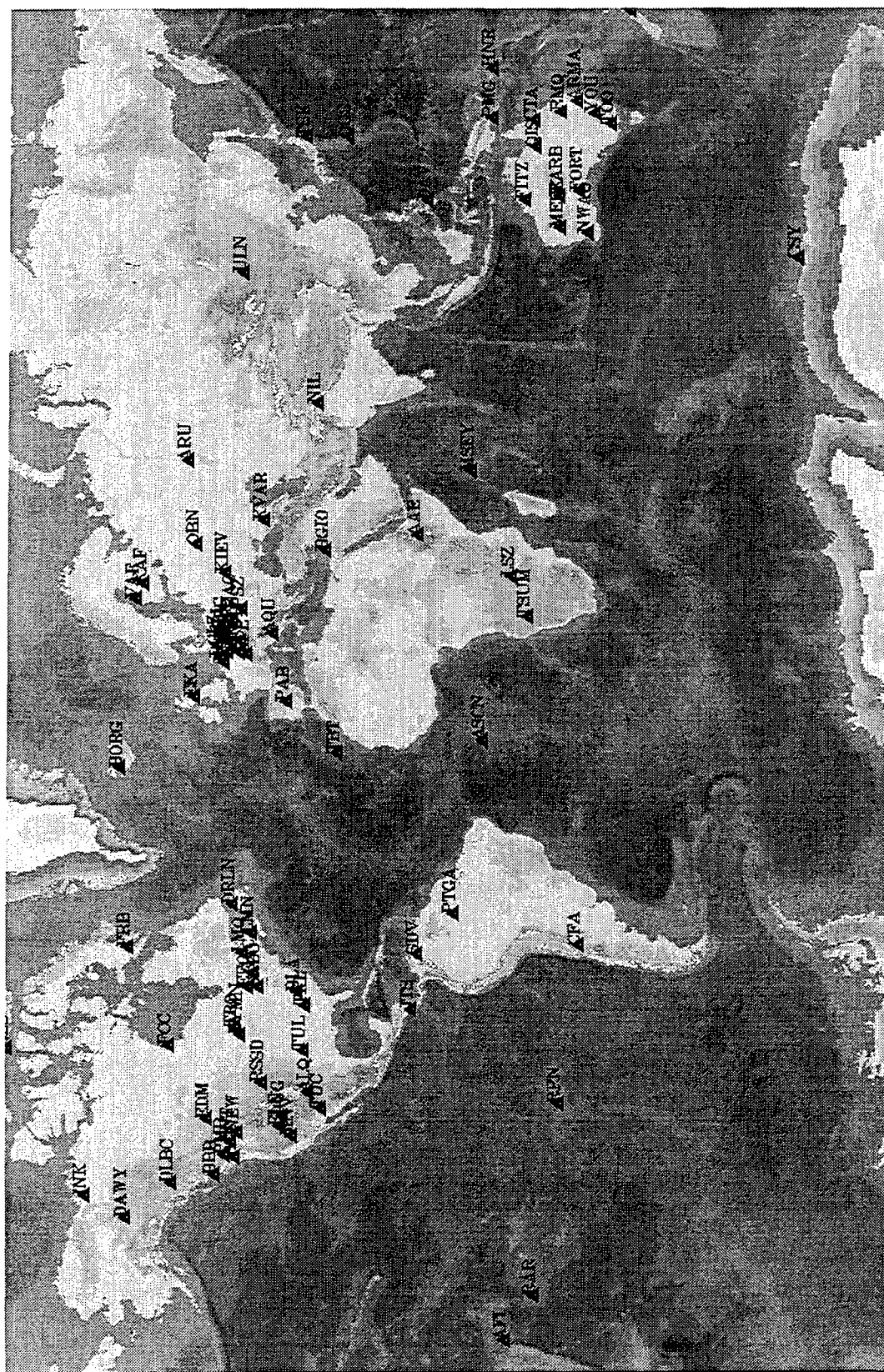


Figure 1. Location of IDC primary stations participating in GSETT-3.



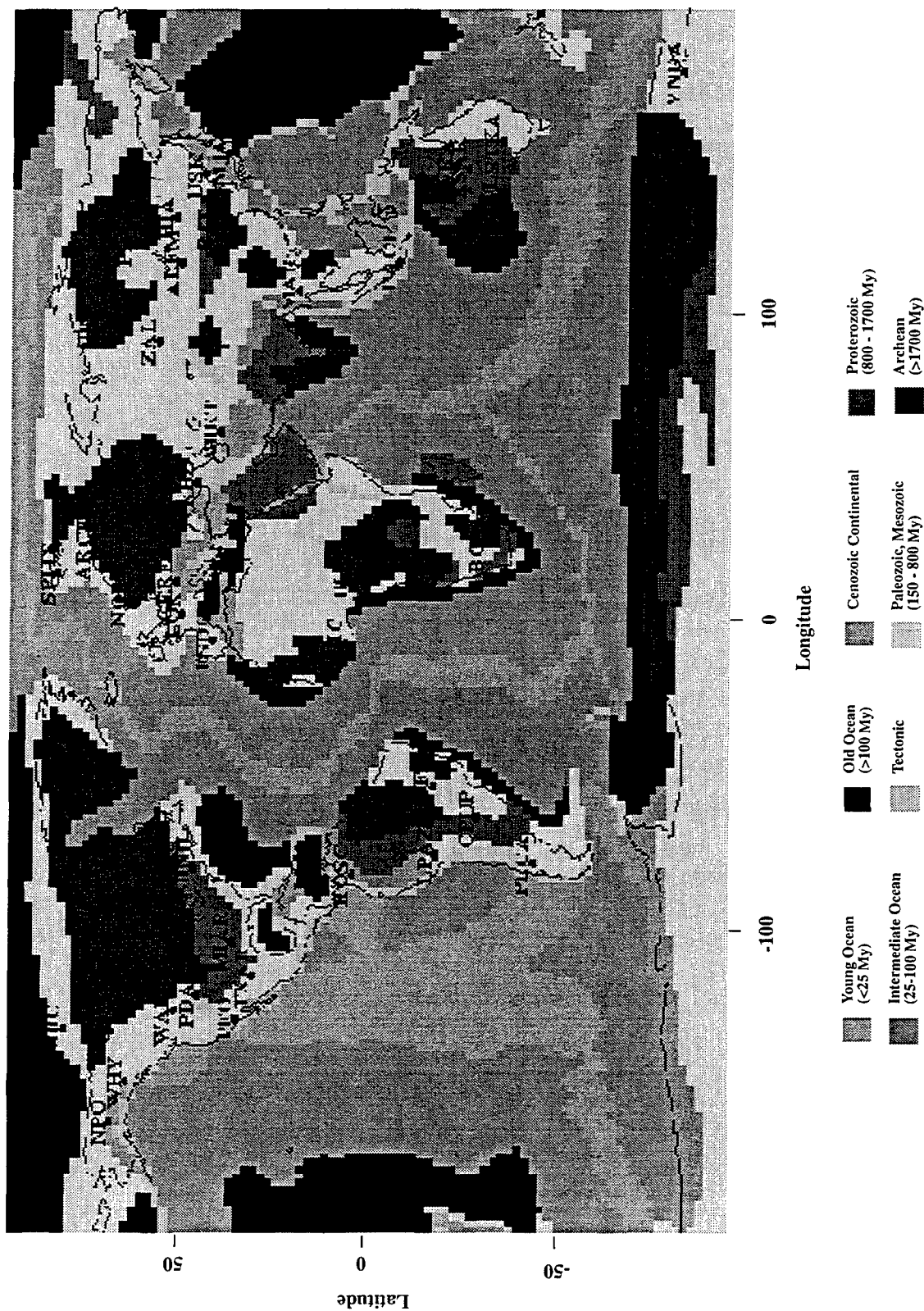


Figure 3. Tectonic regionalization map showing locations of IDC primary stations. This tectonic map is based on a 2° by 2° grid provided by O. Gudmundsson of the Australian National University [personal communication].

Archean into a single "stable" category and consider this and "tectonic" as our only categories of interest.

2.1.3 Availability of Regional Phases

The REB is the final product of the Prototype IDC. We query the REB database to determine the number of regional phases that are available for each subnetwork defined in Section 2.1.1. We use the following constraints to limit our query to regional events recorded by stations in the subnetwork:

- Origin time between January 1, 1995 and June 1, 1996
- Associated regional phases in the REB (e.g., Pn, Pg, Sn, Lg)
- Distance less than 20°
- Depth less than 40 km

We examine the quantity of regional arrivals, the availability of multiple-station associations, and the tectonic environment for each subnetwork. The results are summarized in Table 1. Table A1 in Appendix A provides more detail on the statistics for each station in each subnetwork.

Table 1: SubNetworks of IDC Primary and Auxiliary Stations.

SubNetwork	Pn	Pg	Sn	Lg	Multiple-Station Events	Tectonic Name	Stations
E. Caucasus/Hindu Kush/ E. Med. Sea	262	27	81	35	14	Tectonic	ABKT, KBZ, KVAR, NIL, BGIO
Pacific Rim	1299	60	402	93	240	Tectonic	MJAR, OGS, TSK
Spain	273	23	62	67	60	Tectonic	ESDC, PAB
Thailand	265	86	23	84	0	Tectonic	CMAR
Western USA / Western Canada	1150	334	227	502	267	Tectonic	PDAR, PFO, WALA, BBB, DUG, EDM, ELK, MNV, NEW, PGC, PMB, PNT, RSSD, TUC
Alaska/NW Canada	1315	154	440	438	285	Mixed	WHY, YKA, NPO, MBC, DAWY, DLBC, INK
Central Africa	53	1	29	12	0	Mixed	BGCA, DBIC, AAE
South America	642	12	105	70	175	Mixed	BDFB, CPUP, LPAZ, PLCA, ROSC
Antarctica	39	0	22	9	0	Stable	MAW, VNDA, CSY
Australia	3683	75	2064	339	1028	Stable	ASAR, STKA, WOOL, WRA, ARMA, CTA, FITZ, FORT, MEEK, NWAQ, QIS, RMQ, TOO, WARB, YOU
Central Asia	197	21	71	84	19	Stable	ALFM, BJT, HIA, NRI, PDY, ZAL, ARU, ULN, USK
North American Shield	452	34	159	159	54	Stable	LBNH, SCHQ, ULM, DRLN, EEO, EYMN, FCC, FRB, GAC, LMN, LMQ, RES, SADO, TBO
South Africa	48	15	31	38	9	Stable	BOSA, LSZ, TSUM
Southern USA	551	60	75	190	133	Stable	MIAR, TXAR, AIQ, TKL, TUL

Several subnetworks have a sufficient number of regional arrivals for our attenuation study (Australia, Pacific Rim, Alaska/NW Canada, Western USA/Western Canada, South America, Southern USA, and North America Shield). The Central Asia, Thailand, E. Caucasus/Hindu Kush/E. Med. Sea, and Spain subnetworks may have enough regional phases, but may require more depending on the geographic distribution. Other subnetworks such as Central Africa, South Africa, and Antarctica do not appear to have enough regional phases in the REB. There may be additional regional phases recorded at these stations, but the events do not appear in the REB because they do not satisfy the GSETT-3 event confirmation criteria. Many National Data Centers (NDCs) provide event bulletins based on local networks (called Gamma bulletins) to the IDC. As described in the next section, these local events can be used to supplement our data sets.

Table 1 shows that excellent coverage is available for most "stable" regions, and several of the tectonic regions. Several of the subnetworks have stations in both stable and tectonic environments, and we classify these subnetworks as "mixed." We will develop attenuation models for each subnetwork, and then combine data from several subnetworks to derive generalized attenuation models for each tectonic environment (e.g., tectonic and stable).

We may change the subnetworks as we accumulate more data and ground-truth information, but we believe that the 14 subnetworks in Table 1 provide the best possible data sets for the attenuation study. We will chose our final 10 subnetworks from this list.

2.2 Event Selection

We search event bulletins for event and arrival data that will be used for calculating the attenuation models. We use the same selection criteria as our station selection criteria. Waveform data that corresponds to our selected events will come from IDC primary and auxiliary stations.

We also compile data sets that will be used to evaluate the effectiveness of the Lg/P discriminant. These are likely to include the events used to develop the attenuation models, but they must also include others. The attenuation models are based on the highest quality data that are available, but the Lg/P discriminant must be tested on typical events in the REB (i.e., not just the high-quality events).

2.2.1 Attenuation Models

The REB currently includes over 31,000 events and will be the primary source of data for the attenuation models. However, this is supplemented with the other bulletins whenever possible to fill in regions with sparse coverage. Twenty-one National Data Centers (NDCs) from around the world provide event bulletins to the IDC. The compilation of these individual NDC bulletins is called the Gamma bulletin, and we use this bulletin as our main supplemental bulletin. The Gamma bulletin includes many local events that are not in the REB due to strict GSETT-3 event confirmation criteria, the small size of local events, and sparse local IDC network coverage. However, some detections from these smaller events may have been recorded by IDC primary or auxiliary stations. We may consider using other event bulletins such as the Preliminary Determination of Epicenters (PDE) bulletin produced by the United States Geological Survey (USGS) as needed.

For the attenuation models, we must assess the ray-path distribution for each subnetwork. For example, Figure 4 shows Pn, Pg, Sn, and Lg ray-paths for our Australian subnetwork. We use these maps to evaluate whether or not we need to add or subtract data to obtain adequate coverage for a region. In this example, there are many more Pn phases from events originating in the Java Trench to the north than from events to the south or east. We may want to remove some or all of the Java Trench events to avoid biasing our results for paths from that source region. One approach would be to only use data from Java Trench events with high signal-to-noise ratio. Alternately, we may omit events from the Java Trench so that our attenuation estimates are made solely from events within the continent of Australia. We will evaluate which strategy is most effective.

2.2.1.1 Supplemental Bulletins

Adding events and arrivals to our data set from supplemental bulletins may significantly improve coverage in many regions. Table 2 lists the participating NDCs and the current number of events in the Gamma bulletin that were reported during GSETT-3. Figure 5 shows the global distribution of Gamma events that might be used in our inversion. However, in order to determine whether any of these events can be used in our attenuation study, we must develop procedures and criteria to search for the IDC arrivals that are associated with events in the Gamma or other bulletins.

Table 2: Supplemental NDC Bulletins.

Country	National Data Center (NDC)	Number of Events
Australia	AUS	160
Bulgaria	BGR	89
Canada	CAN	475
Switzerland	CHE	26
China	CHN	3138
Germany	DEU	147
Denmark	DMK	3
Spain	ESP	1059
Finland	FIN	1558
France	FRA	281
Great Britain	GBR	34
Hungary	HUN	13
Israel	ISR	37
Italy	ITA	488
Japan	JPN	10110
New Zealand	NZL	3599
Poland	POL	461
Romania	ROM	255
South Africa	RSA	790
Russia	RUS	1916
United States	USA	3007

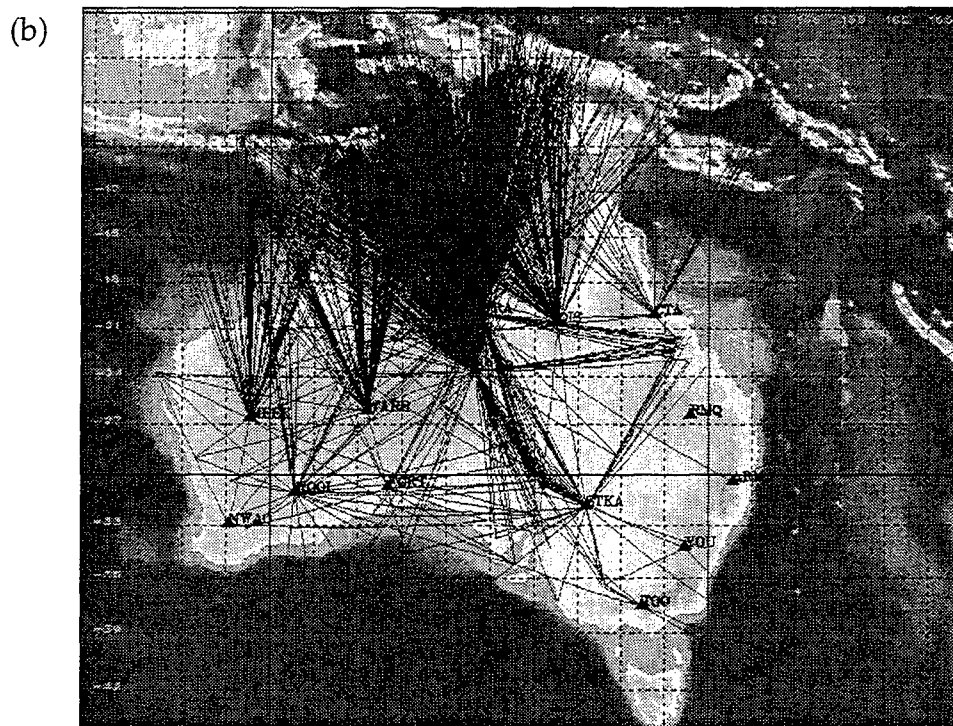
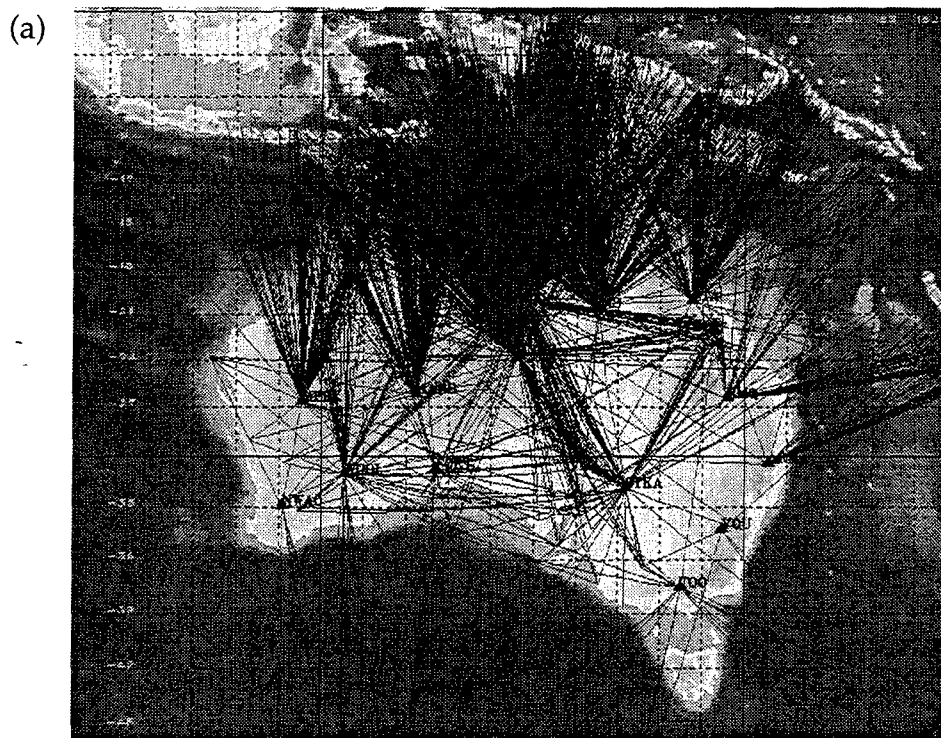


Figure 4. Example from the Australian subnetwork showing regional events recorded by IDC primary and auxiliary stations as reported in the Reviewed Event Bulletin. This data set covers the time period of January 1, 1995 to June 1, 1996. Many more regional phases originate from events to the north than from events to the south or east. (a) Pn, (b) Sn, (c) Pg, and (d) Lg ray-paths.

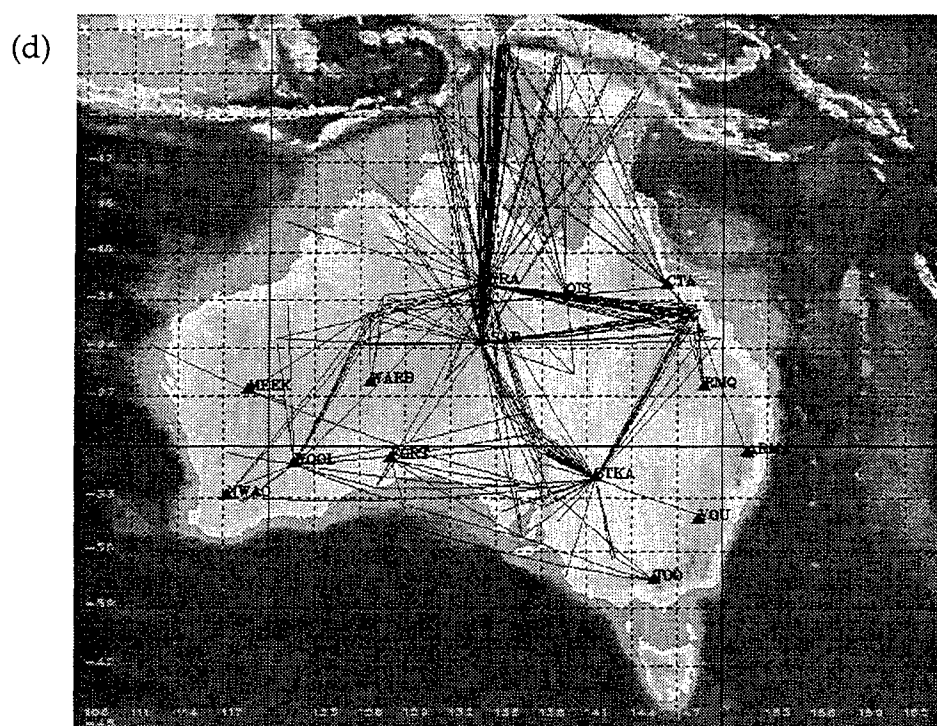
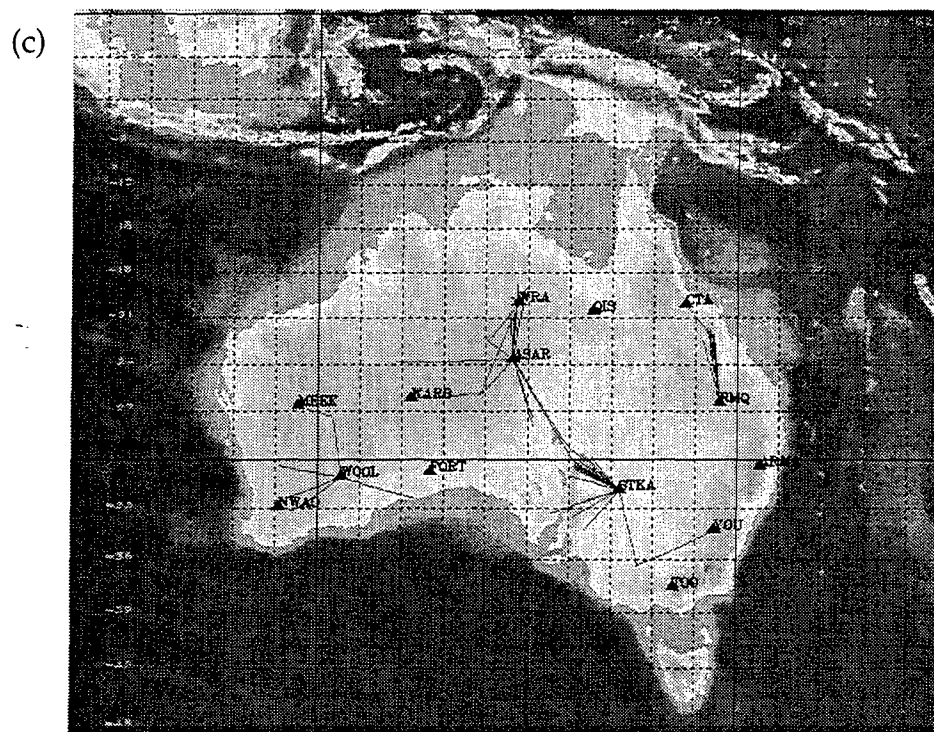


Figure 4. (Continued)

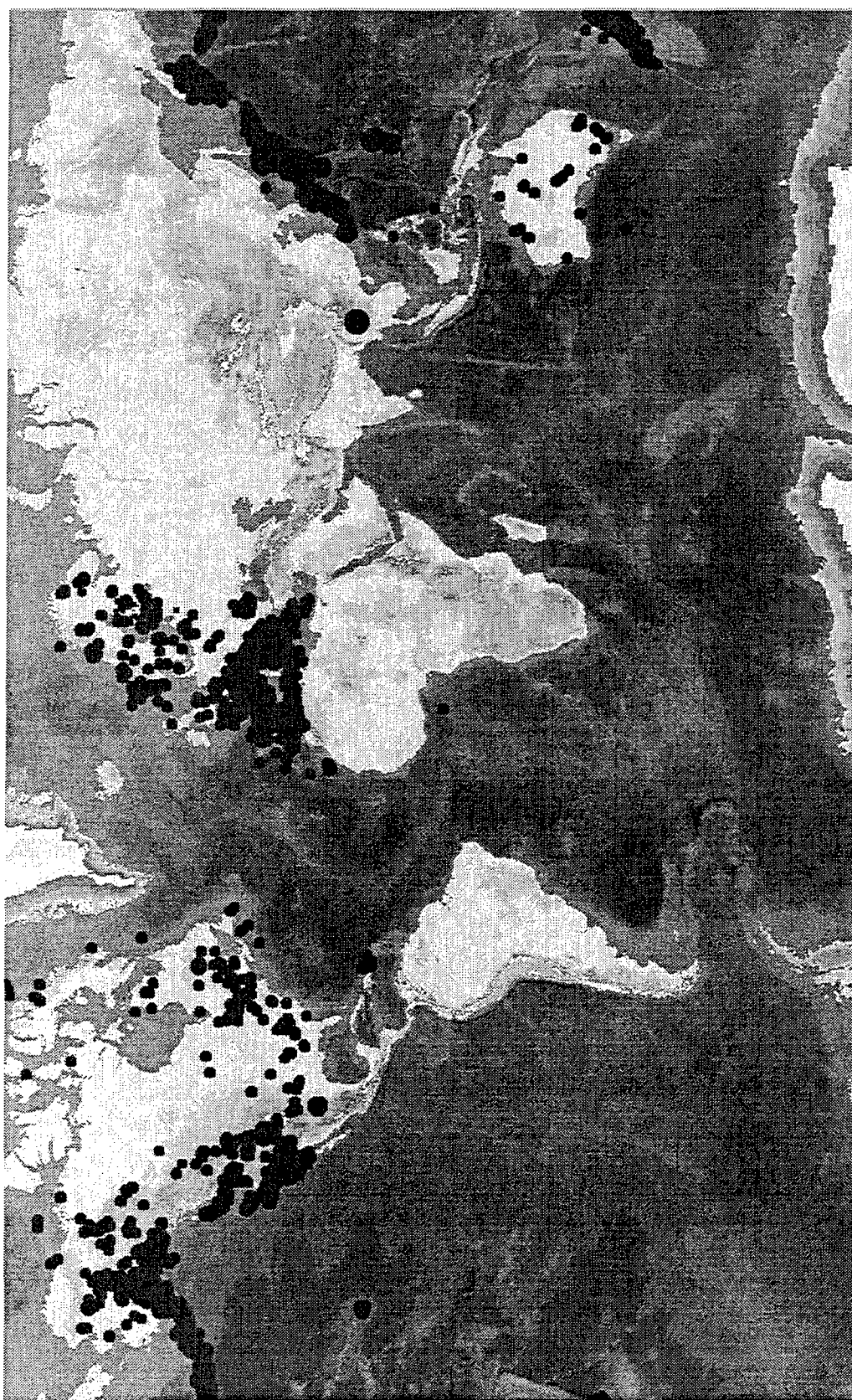


Figure 5. Global distribution of events in the IDC Gamma bulletin.

We use the automated association software at the IDC to associate arrivals in the REB with events in the Gamma bulletin. The software is called the Global Association (GA) system [LeBras *et al.*, 1994]. It uses a data-driven exhaustive grid-search technique, which is based on the generalized beam forming method introduced by Ringdal and Kvaerna [1989].

We consider arrivals that have been detected by the automated system or added by an analyst. Using arrivals from the REB in a 5-minute time interval around the origin time of Gamma events, GA forms event hypotheses over a regional grid around the subnetwork. At each grid point, GA identifies DRIVER arrivals and possible corroborating regional arrivals. A DRIVER is an arrival at one of a limited number of stations in the network that could record the earliest arrival for an event in a given grid cell [LeBras *et al.*, 1994]. GA first constrains the corroborating arrivals using travel time and slowness. A more rigorous chi-square statistical test is applied if an arrival passes this initial screening, and we use all available features of the arrival (travel-time, slowness, azimuth, and amplitude). GA also allows for some of these phases to be identified differently than the initial automated station processing, and eliminates outliers based on a chi-square test of the residuals for each arrival.

After these tests are completed, the event is located using a fixed depth, and an outlier analysis is applied. Outliers are removed if necessary and the location is refined. GA then applies final event confirmation criteria, which include a weighted-count of the number of defining observations, size of the error ellipse major axis, and the probability of detection for events with less than five associations. The probability of detection screens event hypotheses that were detected by an unlikely combination of stations.

As shown in Figure 4a, the Australian region is dominated by events to the north, and additions to the data set from the Gamma bulletin may improve our coverage within the continent. We applied GA to the 160 events provided by the Australian NDC. Of these, 101 are not in the REB. For these non-REB events, we found 44 arrivals in the REB that appear to be associated with 17 regional events. Figure 6 shows the raypaths for the 44 arrivals. Adding these phases will contribute to our coverage of central Australia. The remaining 84 events could not be formed from IDC arrivals due to insufficient data from our primary and auxiliary stations.

We compared the analyst-verified REB associations to those that we obtained for the events in common with both the Gamma bulletin and the REB. When comparing the total number of phases, we obtain a high percentage of associated phases (93%) and defining phases (80%) that are in the REB. Of our defining phases, 82% exactly match the REB defining phases. Thus, we have confidence that our procedure is valid since it produced very similar association sets and locations for events in common with the REB.

2.2.2 Lg/P Discriminant

We will assemble two test data sets to evaluate the effectiveness of the Lg/P discriminant for each subnetwork. The first data set will consist of events whose identifications are known with high confidence, and we call it the *ground-truth* data set. It will be assembled by searching event bulletins that identify source type. The Gamma bulletin will be used for the *ground-truth* data set, since many events are identified (mine blast, explosion,

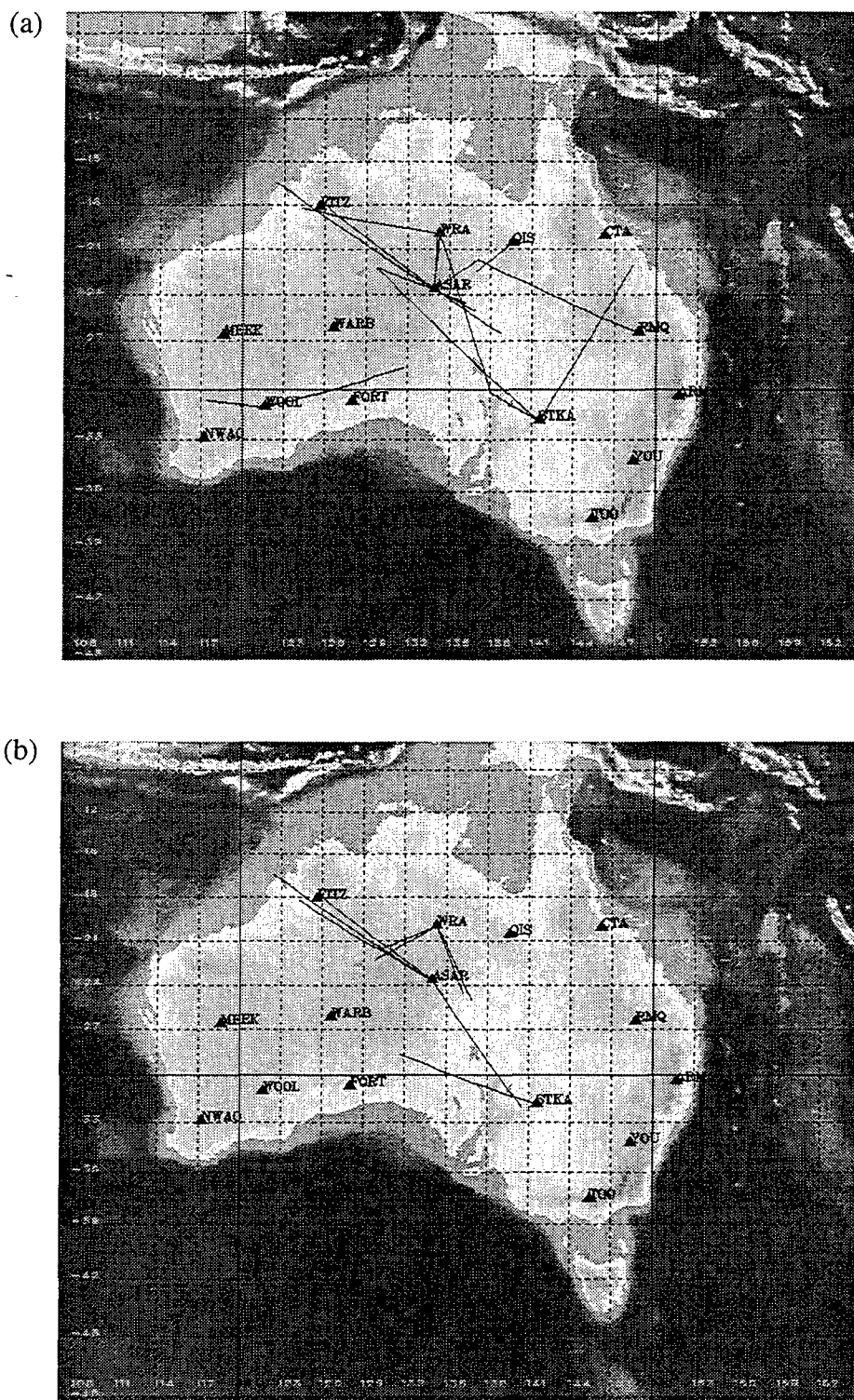


Figure 6. Ray paths for arrivals associated with the Gamma bulletin provided by the Australian National Data Center (NDC). (a) Pn, (b) Sn, (c) Pg, and (d) Lg.

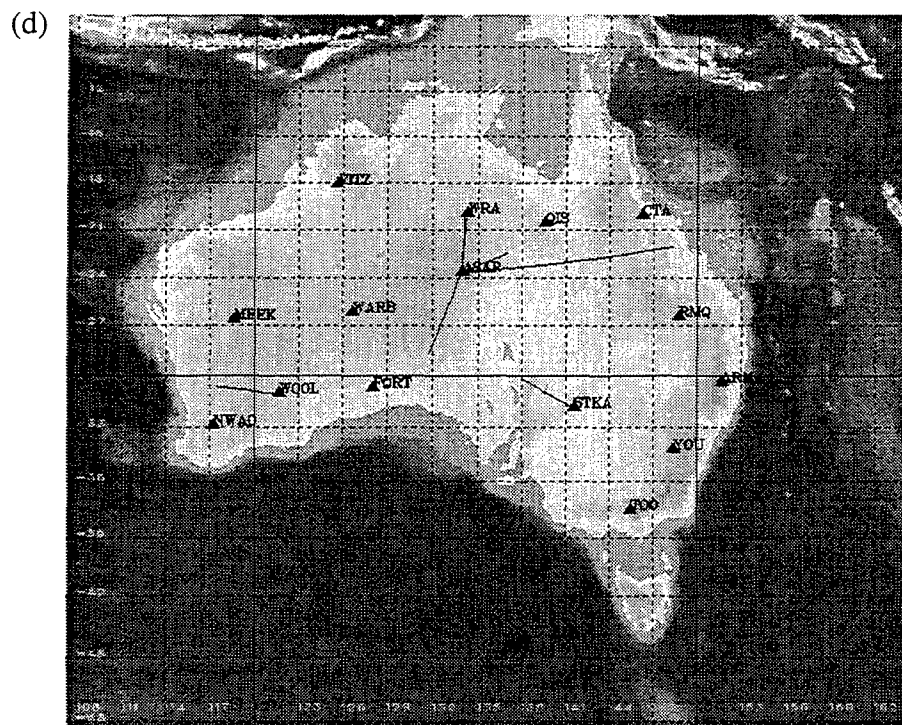
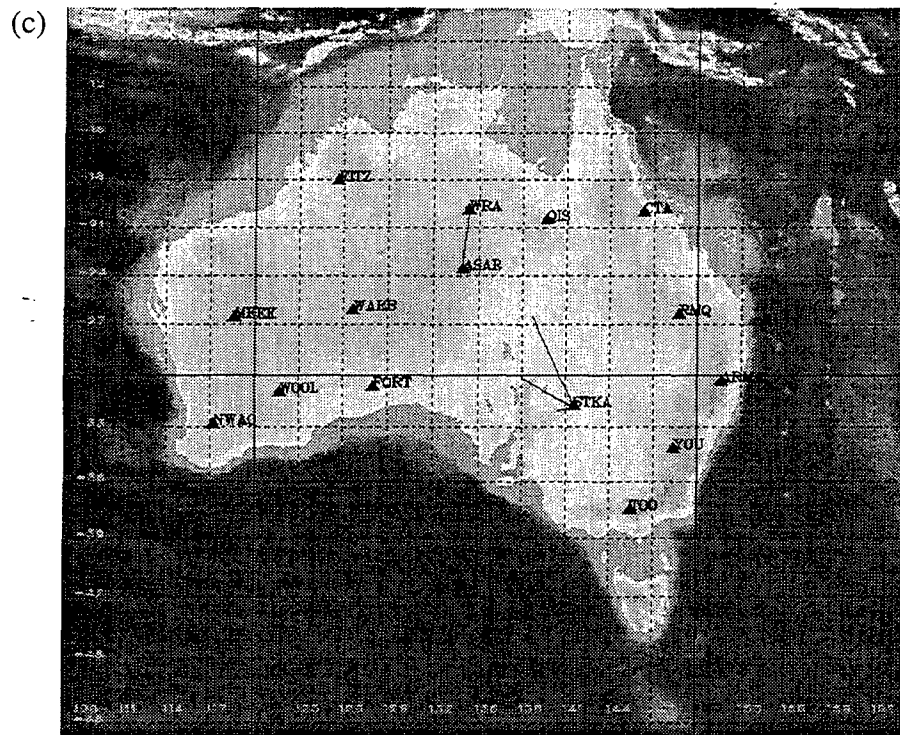
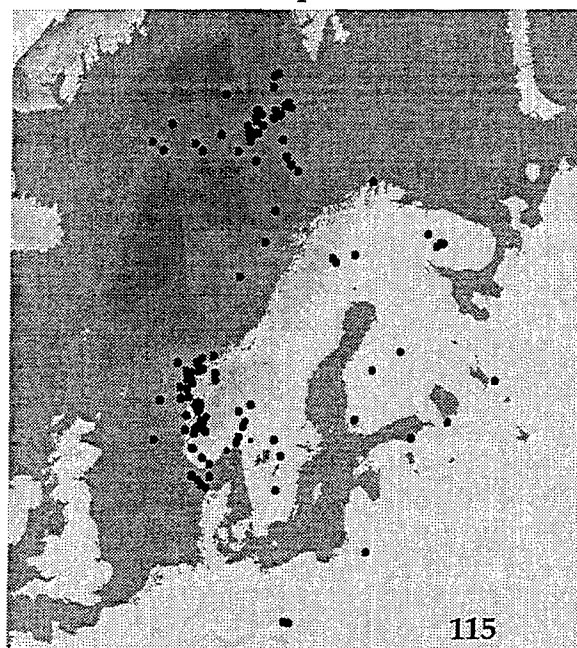


Figure 6. (Continued)

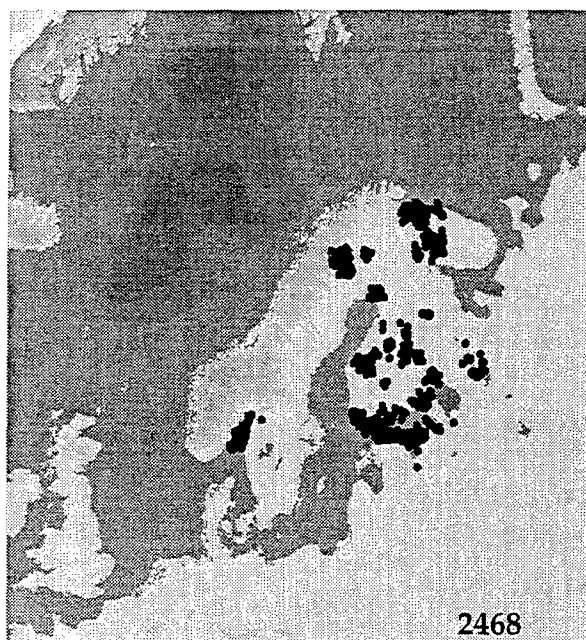
earthquake, etc.). However, we expect that we will need to supplement this with other *ground-truth* information from participating NDCs.

The second data set will include a large number of events (>200 per subnetwork) intended to represent the type of events that are routinely identified by a seismic monitoring system. In general, we will not have *ground-truth* information for these events. Instead, we will rely on knowledge of the local natural and industrial seismicity to qualitatively evaluate the effectiveness of the Lg/P discriminant. We will use the approach developed by *Sereno and Wahl* [1993] for evaluating the Event Identification System in ARPA's Intelligent Monitoring System (IMS). They used knowledge of the local natural and industrial seismicity to qualitatively evaluate the effectiveness of discriminants. Figure 7 shows an example of results using this approach. All of the events that were identified as mine blasts occurred in areas of active mining. Most of the events that were identified as earthquakes are in areas with the highest natural seismicity in this region (the southwest coast of Norway and the Mid-Atlantic Ridge). Many of the events that were identified as explosions are in active mining areas, but the case-based approach used in the IMS failed to associate them with a known mine. Several of the offshore clusters are known to be explosions from military exercises. Some of the events are obviously identified incorrectly by the automated system (such as the events that were identified as explosions on the Mid-Atlantic Ridge). However, this example shows how we can gain valuable information regarding the performance of a discriminant (or set of discriminants) using the general properties of a large sample of events without *ground-truth* information.

Earthquakes



Mine Blasts



Explosions (ML > 2.0)



Figure 7. These maps show the location of events that were identified as earthquakes, mine blasts and explosions by the IMS Event Identification System. Ground-truth information is not available for these events, but it is clear that most of the events are identified correctly. The number of events is listed in the lower right corner of each map.

3. Attenuation Models

We will estimate frequency-dependent attenuation of regional phases recorded by up to 10 IDC subnetworks. We measure amplitudes of regional phases, and develop software to invert them for source and attenuation models. Figure 8 shows the major software components. DFX was developed for the PIDC to perform seismic signal detection and feature extraction. It will be used in this study to compute regional wave amplitudes in the time- and frequency-domains. AmpInv is a new program being developed under this contract to invert the regional wave amplitudes for source and attenuation parameters.

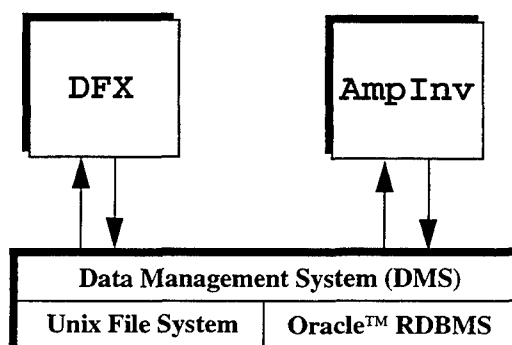


Figure 8. DFX and AmpInv are the two major software components for this project. Both programs interface with the IDC's Data Management System.

3.1 Amplitude Measurements

The software program DFX (Detection and Feature eXtraction) was developed for the PIDC to perform seismic signal detection and feature extraction [Wahl, 1996]. For this project, we added the capability for DFX to compute amplitude spectra.

We investigate three types of time-domain amplitude measurements for both 3-component and array stations. These are root mean-square (*rms*), short-term average (*stav*), and the average of absolute amplitude in the time window after removing the *rms*. The *rms* measurements have been used in regional magnitude estimation and explosion yield studies because they provide stable amplitude estimates for regional phases [e.g., Ringdal, 1983; Nuttli, 1986a,b; Israelsson, 1992]. We evaluate the different amplitude measures by comparing the variance with respect to our derived attenuation models. Our preferred amplitude measurement for each phase is the one with the lowest variance.

Measurements are made on both coherent and incoherent beams in up to seven overlapping frequency bands (each one octave wide) from 0.5 Hz to 16.0 Hz. We use 10-second signal windows for Pn, Pg, and Sn starting 0.3 seconds before the analyst-verified onset time in the REB. A group velocity window of 3.0-3.6 km/sec is used for Lg. Noise windows are 5.0 seconds and start 5.5 seconds prior to the signal window. We calculate spectra by demeaning and cosine-tapering the windowed data and applying an FFT. For array stations, the spectra are array-averaged using the method of Bache *et al.* [1985].

Measurements will be made on vertical data channels, but we may evaluate other channels in the future (e.g, radial, transverse, and combined horizontal).

Frequencies with adequate signal-to-noise ratio (*snr*) are determined for each phase. Determination of the frequency limits is bounded by the instrument response at the recording station and limits provided by the user. The *snr* is required whether time- or frequency-domain amplitude measurements are used. For the time-domain, we simply compare the *snr* to the user-specified threshold. For the frequency-domain (i.e. amplitude spectra), we smooth the signal and noise curves and resample them at a coarse sampling rate specified by a user-parameter. The *snr* of each sample must exceed the threshold before that sample can be used in the inversion.

We have computed approximately 6000 amplitude measurements for regional phases recorded at Australian stations. As an example, Figure 9a shows a regional seismogram recorded by the Alice Springs array (ASAR) in Australia from an $M_L=3.6$ event in south-central Australia at a distance of about 500 km. The analyst-reviewed onset times are superimposed. We use a group velocity window for Lg based on epicentral distance and estimates of the event origin time. Figure 9b shows that this time window captures most of the analyst-reviewed Lg onset times. It shows arrival times for 210 Lg arrivals recorded by stations in Australia. Amplitude spectra are computed using the same time windows as those used for time-domain measurements. Figure 9c shows smoothed and instrument-corrected signal and noise spectra for the Pn arrival in Figure 9a. We use these spectra to determine which frequencies to include in the inversion.

3.2 Inversion Method and Software

We use the method of estimating attenuation developed by *Sereno* [1990]. Briefly, the frequency-dependent (either time-domain or spectral) amplitude of the k th wave recorded at the i th station from the j th source is parameterized as:

$$\log A_{ijk}(f) = \log A_{jk}^0(f) + B_k(\Delta_{ij}, \Delta_0, f) + \delta_{ik} \quad (1)$$

where $A_{jk}^0(f)$ is the amplitude at a reference distance Δ_0 , $B_k(\Delta_{ij}, \Delta_0, f)$ is the attenuation from the reference distance to the epicentral distance Δ_{ij} , and δ_{ik} is a station correction. The amplitude at the reference distance is expressed in terms of the material properties at the source and the receiver, source parameters such as the seismic moment, the shape of the source spectrum, and a wave-dependent excitation factor. We use the *Mueller and Murphy* [1971] and *Brune* [1970, 1971] models to parameterize the shape of the source function.

The attenuation is parameterized in terms of a power-law distance dependence with a frequency-dependent exponent:

$$B_k(\Delta_{ij}, \Delta_0, f) = -\log e \cdot \alpha_k^0 \cdot f + n_k(f) \cdot \log(\Delta_0/\Delta_{jk}) \quad (2)$$

where the first term accounts for attenuation from the source to the reference distance, and the second term is the total attenuation from the reference distance to the epicentral distance. The total attenuation includes geometrical spreading, scattering and anelasticity. It is difficult to separate these terms since the geometrical spreading of regional phases is a

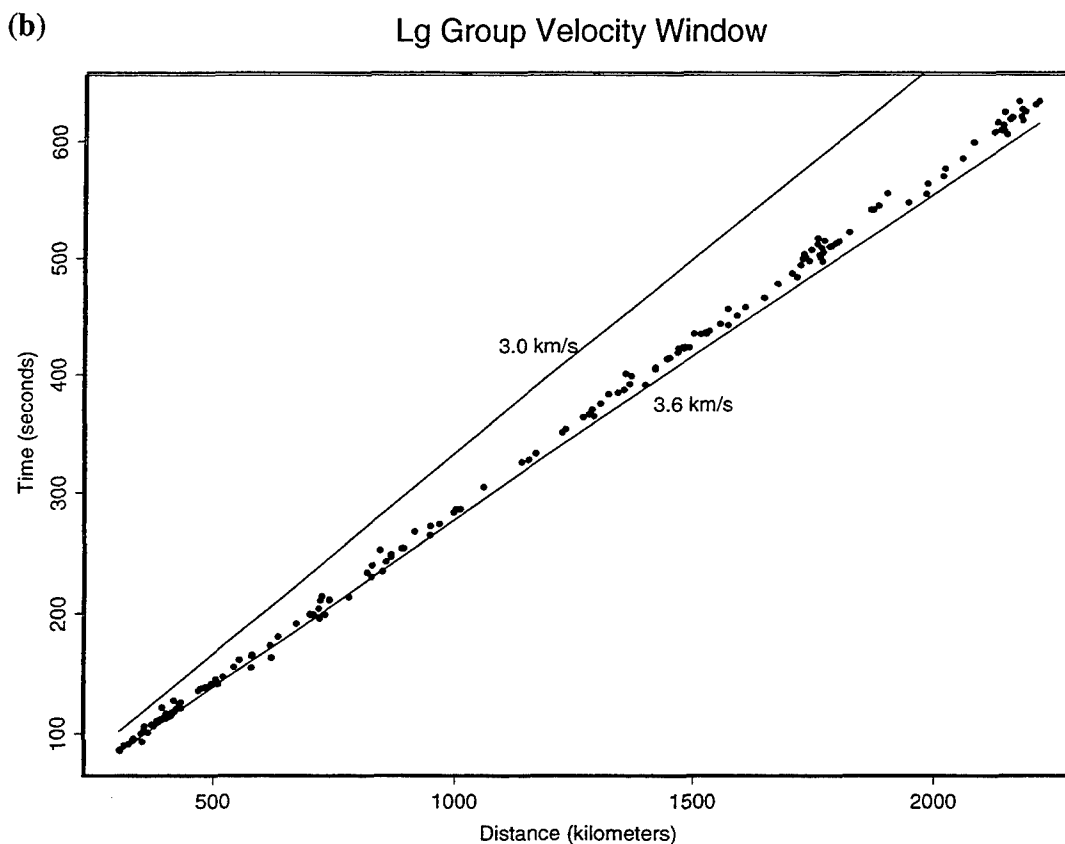
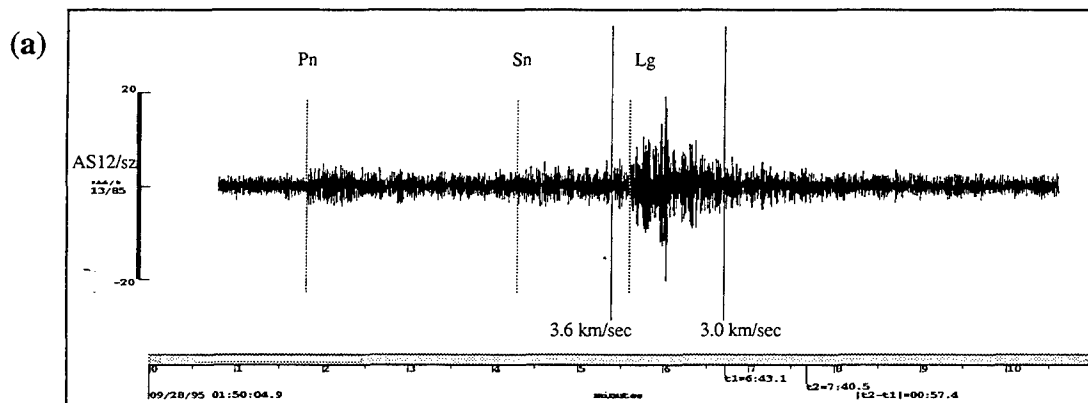


Figure 9. (a) Example of a waveform from one of the elements of the ASAR array. The majority of the Lg energy is included in the 3.0-3.6 km/s group velocity window. (b) Arrival times for 210 Lg phases in the IDC database recorded by stations in Australia. Most arrivals are included in the 3.0-3.6 km/s group velocity window. (c) Signal and noise amplitude spectra for the Pn arrival shown in (a).

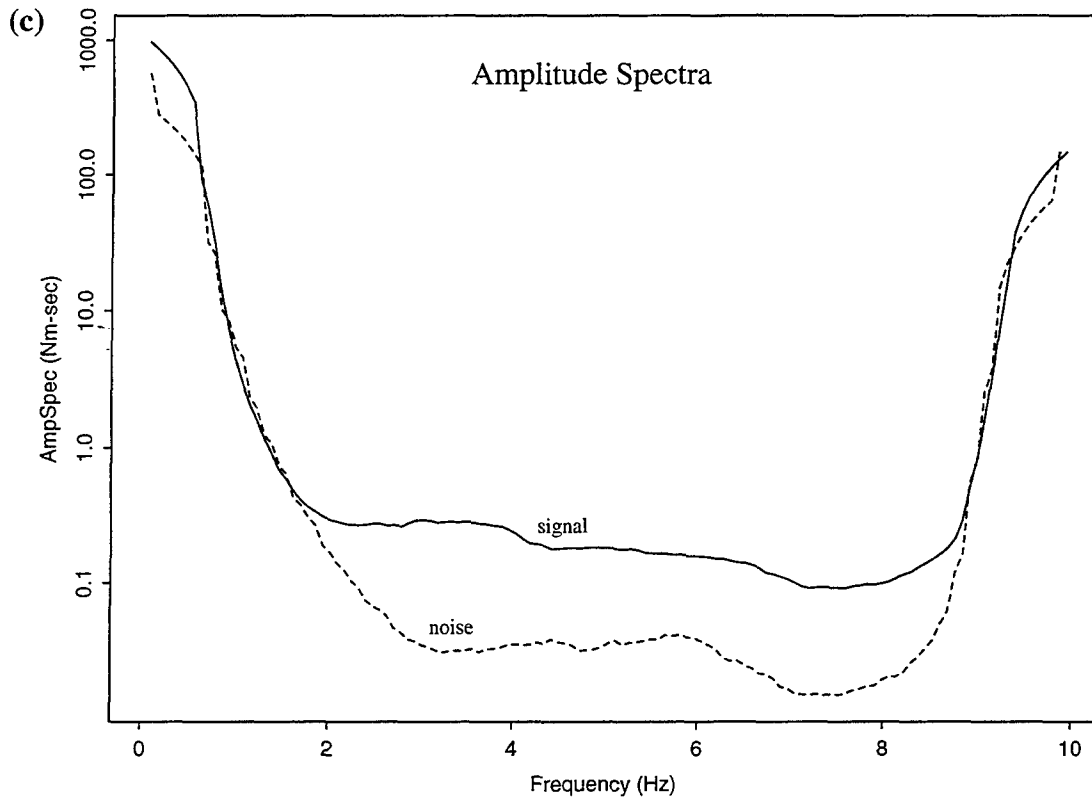


Figure 9. (Continued)

complicated function of the crustal and upper mantle velocity structure [e.g., *Sereno and Given*, 1990]. Fortunately, it is not important to separate these terms for application to the Lg/P discriminant. The exponent, $n_k(f)$, is parameterized as a linear function of frequency.

The system of equations governing the relationship between the data (log amplitudes) and model parameters is formulated by subtracting theoretical data computed from an assumed starting model from the observed data, and solving iteratively for the model perturbations that minimize the data residuals in a least-squares sense. The inversion process is described in detail in Figure 10. We calculate the data residual (*dres*) between the observed data (*dobs*) and data predicted (*dpre*) based on the starting model (*M*). Next, we create the partial derivative matrix containing the system of equations (*G*) describing our problem and then decompose it by a singular value decomposition (SVD) as outlined by *Stewart and Leyk* [1994]. The decomposition yields eigenvector matrices for the model (*V*) and data (*U*), and also calculates a matrix of singular values (Λ). Damping is applied as a function of the condition number of the singular values as required. The degree of damping is controlled by the magnitude of the condition number. The model perturbation, δm , is determined as:

$$\delta m = V * \Lambda^{-1} * U^T * dres \quad (3)$$

where *V* is the matrix of model eigenvectors, Λ^{-1} is the inverse of singular values matrix, U^T is the transpose of the matrix of data eigenvectors, and *dres* is the data residuals. We

add the model perturbation to the model and proceed with the next iteration. This continues until convergence. Our convergence criteria are based on the maximum number of iterations, the condition number of the singular values matrix (Λ), and a data variance threshold.

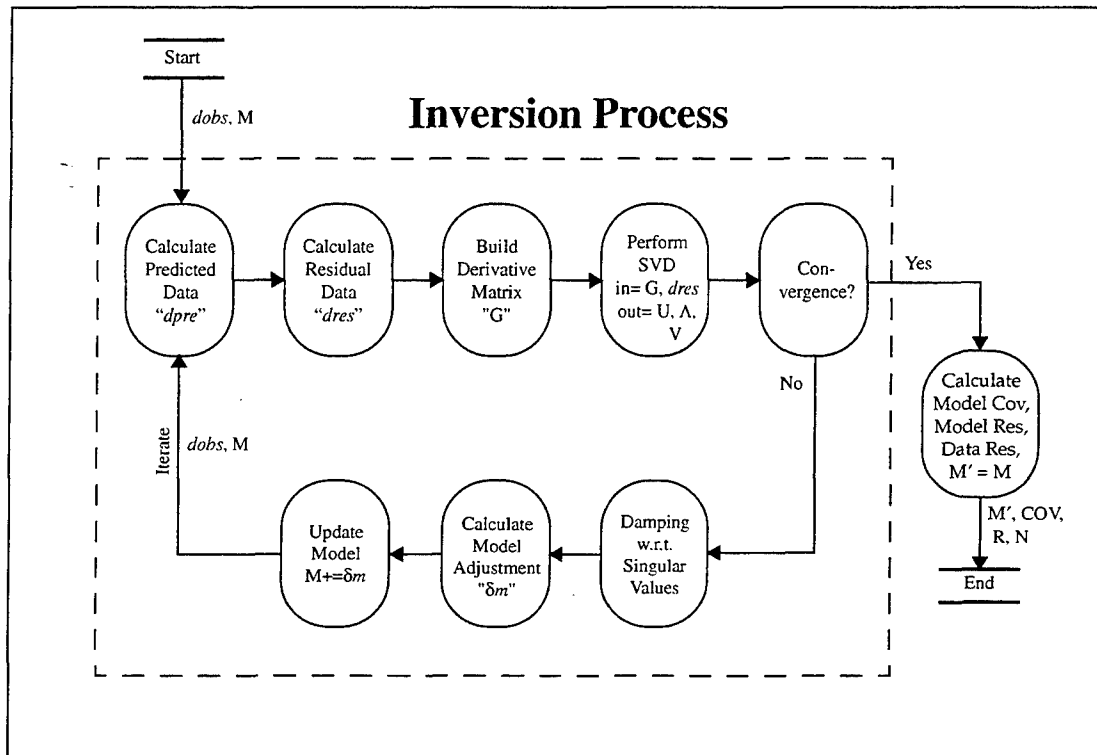


Figure 10. The inversion process receives an observed data set (dobs) and a starting-model (M). A singular value decomposition (SVD) method is used to obtain data eigenvector (U), model eigenvector (V), and singular value (Λ) matrices. Adjustments are made to the model (δm) until the convergence criteria are met. Then, the final model (M'), and model covariance (Cov), model resolution (R), and data resolution (N) matrices are returned.

AmpInv is a new software program that we are developing to implement the inversion method described above (Figure 11). It will invert frequency-dependent amplitudes for source and attenuation parameters such as the long-period source level, a scaling parameter relating corner frequency to long-period source level, phase-dependent excitation factors, anelastic attenuation from the source to a reference distance, total attenuation from the reference distance to receiving station, and a phase-dependent station correction [Sereno, 1990]. AmpInv also generates synthetic amplitudes with or without random noise. We will use synthetic amplitudes to validate AmpInv, experiment with user parameters (e.g., convergence criteria), and evaluate the resolution of source and attenuation parameters for each data set. AmpInv obtains event and amplitude information directly from the DMS using a connection through our Generic Database Interface [Anderson et al., 1994]. The time-domain amplitudes are stored in an OracleTM Relational Database Management System [Swanger et al., 1993], and the amplitude spectra are stored as Unix files on disk.

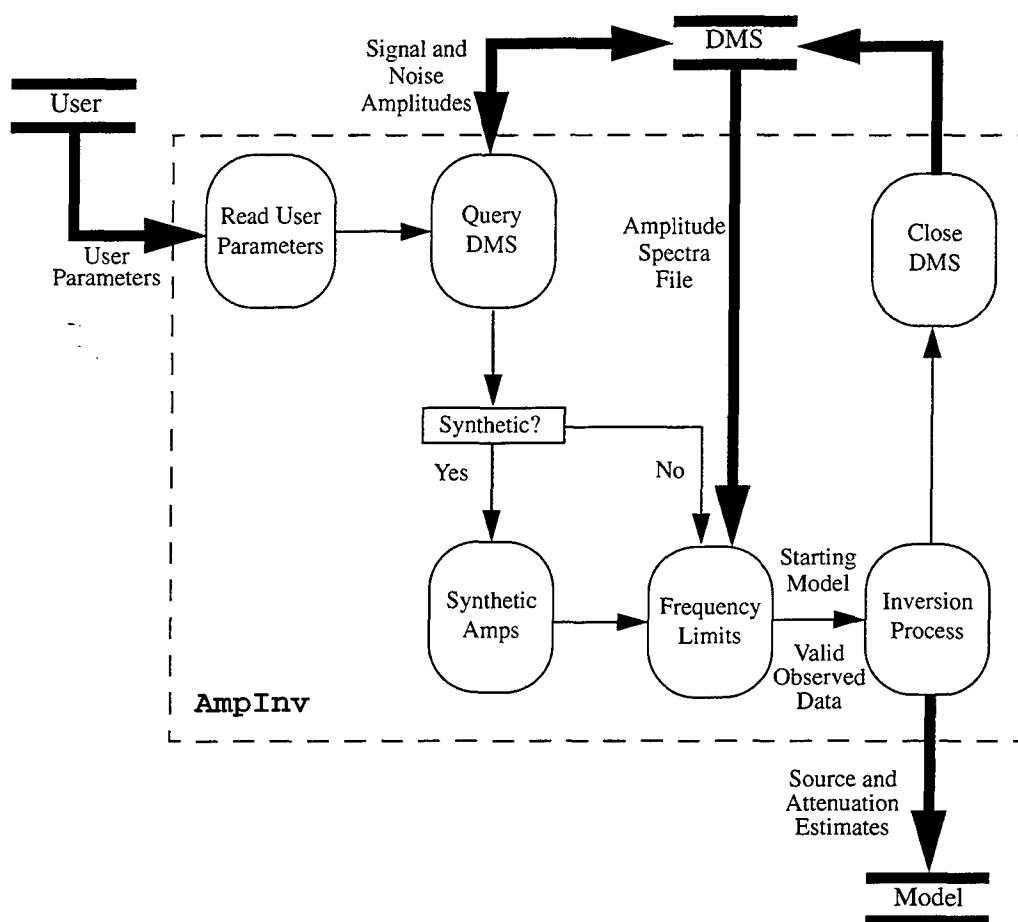


Figure 11. AmpInv process flow diagram. Thin lines link main functional units within AmpInv. Thick lines show interaction with user parameters, the Data Management System (DMS), and output model file.

The User's Guide for AmpInv gives a detailed description of the user parameters, algorithms, and data structures [Jenkins, 1996]. User parameters including database, signal-to-noise limits, phase dependent thresholds, starting model and other parameters that control AmpInv are normally stored in a parameter (or *par*) file, but can also be specified on the command-line. AmpInv reads user input, queries the IDC Data Management System (DMS) for input data, computes synthetic amplitude if desired, determines usable frequency bands for each arrival, inverts for source and attenuation parameters using the inversion process in Figure 10, and writes an output model.

4. Summary and Future Work

During the first year of this two-year project, we developed all software needed for this study, investigated alternative amplitude measures, and compiled a data set for an Australian subnetwork. During the second year, we will compile the data sets for the other IDC subnetworks, estimate regional wave attenuation using `AmpInv`, and evaluate the accuracy and transportability of the Lg/P discriminant. We will also obtain “ground-truth” identification for as many of the events as possible, and we will use knowledge of the local natural and industrial seismicity when this information is not available.

References

- Anderson, J., M. Mortell, B. MacRitchie, and H. Turner, Generic Database Interface (GDI) User Manual, *Tech. Rep. SAIC-93/1001*, Science Applications International Corporation, 1994.
- Bache, T., P. Marshall, and L. Bache, Q for teleseismic P waves from central Asia, *J. Geophys. Res.*, 90, 3575-3587, 1985.
- Baumgardt, D., and G. Young, Regional seismic waveform discriminants and case-based event identification using regional arrays, *Bull. Seismol. Soc. Am.*, 80, 1874-1892, 1990.
- Baumgardt, D., J. Carney, M. Maxson and S. Carter, Evaluation of regional seismic discriminants using the Intelligent Seismic Event Identification System, *Tech. Rep. SAS-TR-93-38*, ENSCO, Inc., Springfield, Virginia, 96 pp., 1992.
- Bennett, J., and J. Murphy, Analysis of seismic discrimination capabilities using regional data from western United States events, *Bull. Seismol. Soc. Am.*, 76, 1069-1086, 1986.
- Bennett, J., B. Barker, K. McLaughlin, and J. Murphy, Regional discrimination of quarry blasts, earthquakes, and underground nuclear explosions, *Final Rep. GL-TR-89-0114*, 146 pp., 1989, ADA223148
- Bennett, J., A. Campanella, J. Scheimer, and J. Murphy, Demonstration of regional discrimination of Eurasian seismic events using observations at Soviet IRIS and CDSN stations, *Final Rep. PL-TR-92-2090*, 122 pp., 1992, ADA253275
- Bennett, J., J. Scheimer, A. Campanella, and J. Murphy, Seismic characteristics of rockbursts for use in discrimination, *Sci. Rep. PL-TR-93-2059*, 89 pp., 1993, ADA266063
- Blandford, R., Seismic discrimination problems at regional distances, in *Identification of Seismic Sources - Earthquake or Nuclear Explosion*, E. S. Husebye and S. Mykkeltveit (Ed.), D. Reidel Publishing Co., Dordrecht, The Netherlands, 695-740, 1981.
- Brune, J., Tectonic stress and the spectra of seismic shear waves from earthquakes, *J. Geophys. Res.*, 75, 4997-5009, 1970. (Correction, *J. Geophys. Res.*, 76, 5002, 1971).
- Chan, W., R. Baumstark, and R. Cessaro, Spectral discrimination between explosions and earthquakes in central Eurasia, *Tech. Rep. GL-TR-90-0217*, 38 pp., 1990, ADA230048
- Dysart, P., and J. Pulli, Regional seismic event classification at the NORESS array: seismological measurements and the use of trained neural networks, *Bull. Seismol. Soc. Am.*, 80, 1910-1933, 1990.
- Gupta, I., and J. Burnetti, An investigation of discriminants for events in Western USSR based on regional phases recorded at station Kabul, *Bull. Seismol. Soc. Am.*, 71, 263-274, 1981.
- Israelsson, H., RMS Lg as a yield estimator in Eurasia, *Final Rep., PL-TR-92-2117 (I)*, 188 pp., 1992, ADA256692
- Jenkins, R.D., Users's Guide for the Amplitude Inversion Software (AmpInv), *Tech. Rep. SAIC-96/1132*, Science Applications International Corporation, 20 pp., 1996.
- Kerr, A., (ed.), Overview GSETT-3. Report prepared by the GSE Working Group on Planning, 9 pp., October, 1993.

- LeBras, R., H. Swanger, T. Sereno, G. Beall, R. Jenkins, and W. Nagy, Global association design document and user's manual, *Tech. Rep. SAIC-94/1142*, Science Applications International Corporation, 67 pp., 1994.
- Lynnes, C., and R. Baumstark, Phase and spectral ratio discrimination in North America, *Tech. Rep. PL-TR-91-2212(II)*, 68 pp., 1991, ADA246673
- Mueller, R. and J. Murphy, Seismic characteristics of underground nuclear detonations, *Bull. Seismol. Soc. Am.*, 61, 1675-1692, 1971.
- Murphy, J., and J. Bennett, A discrimination analysis of short-period regional seismic data recorded at Tonto Forest Observatory, *Bull. Seismol. Soc. Am.*, 72, 1351-1366, 1982.
- Nuttli, O., On the attenuation of Lg waves in western and central Asia and their use as a discriminant between earthquakes and explosions, *Bull. Seismol. Soc. Am.*, 71, 249-261, 1981.
- Nuttli, O., Yield estimates of Nevada test site explosions obtained from seismic Lg wave, *J. Geophys. Res.*, 91, 2137-2151, 1986a.
- Nuttli, O., Lg magnitudes of selected East Kazakhstan underground explosions, *Bull. Seismol. Soc. Am.*, 76, 1241-1251, 1986b.
- Pomeroy, P., W. Best, and T. McEvelly, Test ban treaty verification with regional data - a review, *Bull. Seismol. Soc. Am.*, 72, S89-S129, 1982.
- Ringdal, F., Magnitudes from P coda and Lg using NORSAR data, *NORSAR Sci. Rep. 2-82/83*, Kjeller, Norway, 1983.
- Ringdal, F. and T. Kværna, A multi-channel processing approach to real time network detection, phase association, and threshold monitoring, *Bull. Seismol. Soc. Am.*, 79, 780-798, 1989.
- Sereno, T.J., Attenuation of regional seismic phases in Fennoscandia and estimates of arrival time and azimuth uncertainty using data recorded by regional arrays, *Tech. Rep. SAIC-90/1472*, Science Applications International Corporation, 115 pp., 1990.
- Sereno, T. and J. Given, Pn attenuation for a spherically symmetric earth model, *Geophys. Res. Lett.*, 17, 1141-1144, 1990.
- Sereno, T. and D. Wahl, A fuzzy logic approach to regional seismic event identification: application to the Novaya Zemlya event on 31 December 1992, *Tech. Rep. SAIC-93/1156*, 24 pp., 1993.
- Stewart, D.E., and Z. Leyk, Meschach: Matrix Computations in C, *Proceedings of The Centre For Mathematics And Its Applications, Vol 32*, Australian National University, 240 pp., 1994.
- Swanger, H., J. Anderson, T.J. Sereno, Jr., J. Given, D. Williams, IMS Extensions to the Center Version 3 Database (Rev. 1), *Tech. Rep. SAIC-93/1123*, Science Applications International Corporation, 103 pp., August 27, 1993.
- Taylor, S., M. Denny, E. Vergino, and R. Glaser, Regional discrimination between NTS explosions and western United States earthquakes at regional distances, *Bull. Seismol. Soc. Am.*, 79, 1142-1176, 1989.
- Wahl, D., Programmer's Guide for the Detection and Feature Extraction Program (DFX), *Tech. Rep. SAIC-96/1069*, Science Applications International Corporation, 77 pp., April 1996.

Willis, D., J. DeNoyer, and J. Wilson, Differentiation of earthquakes and underground nuclear explosions on the basis of amplitude characteristics, *Bull. Seismol. Soc. Am.*, 53, 979-987, 1963.

Wuster, J., Discrimination of chemical explosions and earthquakes in central Europe - a case study, *Bull. Seismol. Soc. Am.*, 83, 1184-1212, 1993.

Appendix A: IDC Primary Station Areas

Table A1 lists the network name, station type (e.g., Pri=primary, Aux=auxiliary), station name, number of regional phases, number of regional and multiple-station events, and the tectonic environment of each member of the network.

Table A1: IDC Primary Station Areas

Subnetwork	Sta Type	Station Name / IDC Name	Pn	Pg	Sn	Lg	Num. Events	Multiple-Station Events	Tectonic Name
Alaska/NW Canada	Pri	Whitehorse, Canada/WHY	305	39	104	101	309	285	Paleo/Mesozoic
		Yellowknife, Canada/YKA	279	13	88	78	285	205	Archean
		North Pole, Alaska/NPO	315	38	103	101	319	243	Cenozoic
		Mould Bay, Canada/MBC	135	4	56	14	135	114	Paleo/Mesozoic
	Aux	Dawson City, Canada/DAWY	190	37	54	72	195	188	Paleo/Mesozoic
		Dease Lake, Canada/DLBC	108	12	33	42	109	104	Paleo/Mesozoic
		Inuvik, Canada/INK	118	15	58	44	118	118	Paleo/Mesozoic
Total			1450	158	496	452			
Antarctica	Pri	Mawson, Antarctica/MAW	19	0	17	0	19	0	Archean
		Vanda, Antarctica/VNDA	13	0	5	2	13	0	Paleo/Mesozoic
	Aux	Casey Station, Antarctica/CSY	7	0	0	7	7	0	Archean
Total			39	0	22	9			
Australia	Pri	Alice Springs, Australia/ASAR	812	15	642	97	823	819	Proterozoic
		Stephens Creek, Aus/STKA	106	20	64	53	106	102	Proterozoic
		Woolibar, Australia/WOOL	78	5	41	18	80	75	Archean
		Warramunga, Australia/WRA	1560	21	961	97	1581	1028	Proterozoic
	Aux	Armidale, Australia/ARMA	38	0	2	1	38	13	Paleo/Mesozoic
		Charters Towers, Australia/CTA	184	1	22	13	188	78	Paleo/Mesozoic
		Fitzroy Crossing, Aus/FITZ	5	0	2	0	5	4	Archean
		Forrest, Australia/FORT	21	0	9	6	23	22	Archean
		Meekathara, Australia/MEEK	126	1	63	4	127	99	Archean
		Narrogin, Australia/NWAO	11	2	4	5	14	11	Archean
		Mt Isa, Australia/QIS	455	0	138	15	457	388	Proterozoic
		Roma, Australia/RMQ	67	8	0	6	66	35	Proterozoic
		Toolangi, Australia/TOO	18	0	7	4	18	11	Paleo/Mesozoic
		Warburton, Australia/WARB	197	1	109	3	198	194	Proterozoic
Young, Australia/YOU	5	1	3	0	6	5	Paleo/Mesozoic		
Total			3683	75	2064	339			

Table A1: IDC Primary Station Areas

Subnetwork	Sta Type	Station Name / IDC Name	Pn	Pg	Sn	Lg	Num. Events	Multiple-Station Events	Tectonic Name
Central Africa	Pri	Bogoin, C. African Rep/BGCA	18	0	16	11	18	0	Archean
		Dimbroko, Ivory Coast/DBIC	30	1	13	1	30	0	Archean
	Aux	Addis Ababa, Ethiopia/AAE	5	0	0	0	5	0	Paleo/Mesozoic
Total			53	1	29	12			
Central Asia	Pri	Mangolia/ALFM	0	0	0	0	0	0	Paleo/Mesozoic
		Baijiatuan, China/BJT	24	3	4	6	24	6	Archean
		Hailar, China/HIA	3	0	0	0	3	1	Paleo/Mesozoic
		Norilsk, Russia/NRI	14	0	5	4	15	14	Archean
		Peleduy, Russia/PDY	62	6	23	33	64	19	Archean
		Zalesovo, Russia/ZAL	59	7	20	23	61	17	Paleo/Mesozoic
	Aux	Arti, Russia/ARU	23	1	14	9	26	6	Paleo/Mesozoic
		Ussuriisk, Russia/USK	0	0	0	0	0	0	Paleo/Mesozoic
		Ulaanbaatar, Mongolia/ULN	12	4	5	9	12	6	Paleo/Mesozoic
Total			197	21	71	84			
East Caucasus/ Hindu Kush/ East Med. Sea	Pri	Alibek, Turkmenistan/ABKT	32	2	13	4	32	10	Cenozoic
		Khabaz, Russia/KBZ	96	8	12	10	97	24	Tectonic
	Aux	Kislovodsk Array, Russia/KVAR	24	3	5	2	25	10	Tectonic
		Bar Giyora, Israel/BGIO	53	3	21	6	55	11	Proterozoic
		Nilore, Pakistan/NIL	57	11	30	13	59	4	Proterozoic
Total			262	27	81	35			
North American Shield	Pri	Lisbon, New Hampshire/LBNH	15	3	6	15	18	18	Proterozoic
		Schefferville, Canada/SCHQ	31	0	12	9	31	17	Archean
		Lac du Bonnet, Canada/ULM	121	13	17	54	126	48	Archean
	Aux	Deer Lake, Canada/DRLN	23	0	6	0	23	4	Paleo/Mesozoic
		Eldee, Canada/EEO	3	1	1	3	3	3	Archean
		Ely, Minnesota/EYMN	6	2	4	5	9	7	Archean
		Fort Churchill, Canada/FCC	56	1	20	26	59	40	Archean
		Iqaluit, Canada/FRB	8	0	6	4	8	8	Archean
		Glen Almond, Canada/GAC	4	3	4	5	6	6	Proterozoic
		Caledonia Mtn., Canada/LMN	2	0	1	1	2	2	Paleo/Mesozoic
La Malbaie, Canada/LMQ	5	0	5	5	8	8	Proterozoic		

Table A1: IDC Primary Station Areas

Subnetwork	Sta Type	Station Name / IDC Name	Pn	Pg	Sn	Lg	Num. Events	Multiple-Station Events	Tectonic Name
	Aux	Resolute Bay, Canada/RES	28	1	14	7	28	7	Paleo/Mesozoic
		Sadowa, Canada/SADO	13	6	6	9	13	13	Proterozoic
		Thunder Bay, Canada/TBO	2	0	1	2	3	3	Archean
Total			317	30	103	145			
Pacific Rim	Pri	Matsushiro Array, Japan/MJAR	956	46	244	71	975	240	Tectonic
	Aux	Ogasawara, Japan/OGS	165	6	53	7	169	133	Tectonic
		Tsukuba, Japan/TSK	178	8	105	15	182	177	Old Ocean
Total			1299	60	402	93			
South Africa	Pri	Boshof, South Africa/BOSA	36	15	22	29	41	9	Archean
	Aux	Lusaka, Zambia/LSZ	2	0	2	2	2	1	Paleo/Mesozoic
		Tsumeb, Namibia/TSUM	10	0	7	7	10	8	Archean
Total			48	15	31	38			
South America	Pri	Brasilia, Brazil/BDFB	4	0	0	0	4	3	Paleo/Mesozoic
		Villa Florida, Paraguay/CPUP	188	0	33	20	188	164	Proterozoic
		La Paz, Bolivia/LPAZ	218	3	34	15	217	73	Paleo/Mesozoic
		Paso Flores, Argentina/PLCA	232	9	38	35	234	175	Tectonic
		El Rosal, Colombia/ROSC	0	0	0	0	0	0	Tectonic
Total			642	12	105	70			
Southern USA	Pri	Mount Ida, Arkansas/MIAR	108	8	22	33	109	89	Proterozoic
		TXAR Array, Texas/TXAR	321	25	31	117	323	133	Paleo/Mesozoic
	Aux	Albuquerque, N M/ALQ	71	18	10	23	74	60	Proterozoic
		Tuckaleechee Caverns, TN/TKL	9	6	4	9	13	9	Proterozoic
		Tulsa, Oklahoma/TUL	42	3	8	8	46	44	Proterozoic
Total			551	60	75	190			
Spain	Pri	Sonseca Array, Spain/ESDC	211	16	41	47	208	60	Paleo/Mesozoic
	Aux	San Pablo, Spain/PAB	62	7	21	20	62	60	Paleo/Mesozoic
Total			273	23	62	67			
Thailand	Pri	Chiang Mai, Thailand/CMAR	265	86	23	84	278	0	Paleo/Mesozoic
Total			265	86	23	84			
Western USA/ Western Canada	Pri	Pinedale Array, WY/PDAR	292	77	38	109	305	267	Paleo/Mesozoic
		Pinon Flat, California/PFO	121	49	24	52	137	128	Tectonic

Table A1: IDC Primary Station Areas

Subnetwork	Sta Type	Station Name / IDC Name	Pn	Pg	Sn	Lg	Num. Events	Multiple-Station Events	Tectonic Name
	Pri	Waterton Lakes, Canada/WALA	202	52	44	108	233	207	Paleo/Mesozoic
	Aux	Bella Bella, Canada/BBB	42	8	24	13	47	37	Paleo/Mesozoic
		Dugway, Utah/DUG	64	25	6	31	71	71	Tectonic
		Edmonton, Canada/EDM	66	10	10	23	72	71	Paleo/Mesozoic
		Elko, Nevada/ELK	25	10	1	13	25	24	Paleo/Mesozoic
		Mina, Nevada/MNV	46	30	12	26	55	55	Paleo/Mesozoic
		Newport, Washington/NEW	35	9	7	19	38	38	Paleo/Mesozoic
		Pacific Geo. Ctr., Canada/PGC	28	4	13	6	31	31	Paleo/Mesozoic
		Pemberton, Canada/PMB	65	10	17	23	66	61	Paleo/Mesozoic
		Penticton, Canada/PNT	65	12	17	24	66	66	Paleo/Mesozoic
		Black Hills, SD/RSSD	21	20	3	22	40	38	Archean
		Tucson, Arizona/TUC	78	18	11	33	86	72	Paleo/Mesozoic
Total			1150	334	227	502			

THOMAS AHRENS
SEISMOLOGICAL LABORATORY 252-21
CALIFORNIA INSTITUTE OF TECHNOLOGY
PASADENA, CA 91125

RALPH ALEWINE
NTPO
1901 N. MOORE STREET, SUITE 609
ARLINGTON, VA 22209

SHELTON ALEXANDER
PENNSYLVANIA STATE UNIVERSITY
DEPARTMENT OF GEOSCIENCES
537 DEIKE BUILDING
UNIVERSITY PARK, PA 16801

LOS ALAMOS NATIONAL LABORATORY
ATTN: TECHNICAL STAFF (PLS ROUTE)
PO BOX 1663, MS F659
LOS ALAMOS, NM 87545

LAWRENCE LIVERMORE NATIONAL LABORATORY
ATTN: TECHNICAL STAFF (PLS ROUTE)
PO BOX 808, MS L-200
LIVERMORE, CA 94551

MUAWIA BARAZANGI
INSTITUTE FOR THE STUDY OF THE CONTINENTS
3126 SNEE HALL
CORNELL UNIVERSITY
ITHACA, NY 14853

RICHARD BARDZELL
ACIS
DCI/ACIS
WASHINGTON, DC 20505

T.G. BARKER
MAXWELL TECHNOLOGIES
P.O. BOX 23558
SAN DIEGO, CA 92123

DOUGLAS BAUMGARDT
ENSCO INC.
5400 PORT ROYAL ROAD
SPRINGFIELD, VA 22151

SANDIA NATIONAL LABORATORY
ATTN: TECHNICAL STAFF (PLS ROUTE)
DEPT. 5791
MS 0567, PO BOX 5800
ALBUQUERQUE, NM 87185-0567

THERON J. BENNETT
MAXWELL TECHNOLOGIES
11800 SUNRISE VALLEY DRIVE SUITE 1212
RESTON, VA 22091

WILLIAM BENSON
NAS/COS
ROOM HA372
2001 WISCONSIN AVE. NW
WASHINGTON, DC 20007

JONATHAN BERGER
UNIVERSITY OF CA, SAN DIEGO
SCRIPPS INSTITUTION OF OCEANOGRAPHY IGPP, 0225
9500 GILMAN DRIVE
LA JOLLA, CA 92093-0225

ROBERT BLANDFORD
AFTAC
1300 N. 17TH STREET
SUITE 1450
ARLINGTON, VA 22209-2308

LOS ALAMOS NATIONAL LABORATORY
ATTN: TECHNICAL STAFF (PLS ROUTE)
PO BOX 1663, MS F665
LOS ALAMOS, NM 87545

LAWRENCE LIVERMORE NATIONAL LABORATORY
ATTN: TECHNICAL STAFF (PLS ROUTE)
PO BOX 808, MS L-207
LIVERMORE, CA 94551

STEVEN BRATT
NTPO
1901 N. MOORE STREET, SUITE 609
ARLINGTON, VA 22209

SANDIA NATIONAL LABORATORY
ATTN: TECHNICAL STAFF (PLS ROUTE)
DEPT. 5704
MS 0655, PO BOX 5800
ALBUQUERQUE, NM 87185-0655

LAWRENCE LIVERMORE NATIONAL LABORATORY
ATTN: TECHNICAL STAFF (PLS ROUTE)
PO BOX 808, MS L-221
LIVERMORE, CA 94551

RHETT BUTLER
IRIS
1616 N. FORT MEYER DRIVE
SUITE 1050
ARLINGTON, VA 22209

SANDIA NATIONAL LABORATORY
ATTN: TECHNICAL STAFF (PLS ROUTE)
DEPT. 5736
MS 0655, PO BOX 5800
ALBUQUERQUE, NM 87185-0655

SANDIA NATIONAL LABORATORY
ATTN: TECHNICAL STAFF (PLS ROUTE)
DEPT. 9311
MS 1159, PO BOX 5800
ALBUQUERQUE, NM 87185-1159

SEAN DORAN
ACIS
DCI/ACIS
WASHINGTON, DC 20505

LAWRENCE LIVERMORE NATIONAL LABORATORY
ATTN: TECHNICAL STAFF (PLS ROUTE)
LLNL
PO BOX 808, MS L-175
LIVERMORE, CA 94551

RICHARD J. FANTEL
BUREAU OF MINES
DEPT OF INTERIOR, BLDG 20
DENVER FEDERAL CENTER
DENVER, CO 80225

MARK D. FISK
MISSION RESEARCH CORPORATION
735 STATE STREET
P.O. DRAWER 719
SANTA BARBARA, CA 93102-0719

PACIFIC NORTHWEST NATIONAL LABORATORY
ATTN: TECHNICAL STAFF (PLS ROUTE)
PO BOX 999, MS K6-48
RICHLAND, WA 99352

LORI GRANT
MULTIMAX, INC.
311C FOREST AVE. SUITE 3
PACIFIC GROVE, CA 93950

CATHERINE DE GROOT-HEDLIN
SCRIPPS INSTITUTION OF OCEANOGRAPHY
UNIVERSITY OF CALIFORNIA, SAN DIEGO
INSTITUTE OF GEOPHYSICS AND PLANETARY PHYSICS
LA JOLLA, CA 92093

PACIFIC NORTHWEST NATIONAL LABORATORY
ATTN: TECHNICAL STAFF (PLS ROUTE)
PO BOX 999, MS K7-34
RICHLAND, WA 99352

LESLIE A. CASEY
DOE
1000 INDEPENDENCE AVE. SW
NN-40
WASHINGTON, DC 20585-0420

DR. STANLEY DICKINSON
AFOSR
110 DUNCAN AVENUE
SUITE B115
BOLLING AFB, WASHINGTON D.C. 20332-001

DIANE I. DOSER
DEPARTMENT OF GEOLOGICAL SCIENCES
THE UNIVERSITY OF TEXAS AT EL PASO
EL PASO, TX 79968

SANDIA NATIONAL LABORATORY
ATTN: TECHNICAL STAFF (PLS ROUTE)
SNL, DEPT. 4115
MS 0329, PO BOX 5800
ALBUQUERQUE, NM 87185-0329

JOHN FILSON
ACIS/TMG/NTT
ROOM 6T11 NHB
WASHINGTON, DC 20505

LAWRENCE LIVERMORE NATIONAL LABORATORY
ATTN: TECHNICAL STAFF (PLS ROUTE)
PO BOX 808, MS L-208
LIVERMORE, CA 94551

ROBERT GEIL
DOE
PALAIS DES NATIONS, RM D615
GENEVA 10, SWITZERLAND

HENRY GRAY
SMU STATISTICS DEPARTMENT
P.O. BOX 750302
DALLAS, TX 75275-0302

I. N. GUPTA
MULTIMAX, INC.
1441 MCCORMICK DRIVE
LARGO, MD 20774

PACIFIC NORTHWEST NATIONAL LABORATORY
ATTN: TECHNICAL STAFF (PLS ROUTE)
PO BOX 999, MS K6-40
RICHLAND, WA 99352

DAVID HARKRIDER
PHILLIPS LABORATORY
EARTH SCIENCES DIVISION
29 RANDOLPH ROAD
HANSCOM AFB, MA 01731-3010

THOMAS HEARN
NEW MEXICO STATE UNIVERSITY
DEPARTMENT OF PHYSICS
LAS CRUCES, NM 88003

DONALD HELMBERGER
CALIFORNIA INSTITUTE OF TECHNOLOGY
DIVISION OF GEOLOGICAL & PLANETARY SCIENCES
SEISMOLOGICAL LABORATORY
PASADENA, CA 91125

ROBERT HERRMANN
ST. LOUIS UNIVERSITY
DEPARTMENT OF EARTH & ATMOSPHERIC SCIENCES
3507 LACLEDE AVENUE
ST. LOUIS, MO 63103

ANTHONY IANNACCHIONE
BUREAU OF MINES
COCHRANE MILL ROAD
PO BOX 18070
PITTSBURGH, PA 15236-9986

THOMAS JORDAN
MASSACHUSETTS INSTITUTE OF TECHNOLOGY
EARTH, ATMOSPHERIC & PLANETARY SCIENCES
77 MASSACHUSETTS AVENUE, 54-918
CAMBRIDGE, MA 02139

ANATOLI L. LEVSHIN
DEPARTMENT OF PHYSICS
UNIVERSITY OF COLORADO
CAMPUS BOX 390
BOULDER, CO 80309-0309

GARY MCCARTOR
SOUTHERN METHODIST UNIVERSITY
DEPARTMENT OF PHYSICS
DALLAS, TX 75275-0395

PACIFIC NORTHWEST NATIONAL LABORATORY
ATTN: TECHNICAL STAFF (PLS ROUTE)
PO BOX 999, MS K7-22
RICHLAND, WA 99352

RICHARD MORROW
USACDA/IVI
320 21ST STREET, N.W.
WASHINGTON, DC 20451

JAMES HAYES
NSF
4201 WILSON BLVD., ROOM 785
ARLINGTON, VA 22230

MICHAEL HEDLIN
UNIVERSITY OF CALIFORNIA, SAN DIEGO
SCRIPPS INSTITUTION OF OCEANOGRAPHY IGPP, 0225
9500 GILMAN DRIVE
LA JOLLA, CA 92093-0225

EUGENE HERRIN
SOUTHERN METHODIST UNIVERSITY
DEPARTMENT OF GEOLOGICAL SCIENCES
DALLAS, TX 75275-0395

VINDELL HSU
HQ/AFTAC/TTR
1030 S. HIGHWAY A1A
PATRICK AFB, FL 32925-3002

RONG-SONG JIH
PHILLIPS LABORATORY
EARTH SCIENCES DIVISION
29 RANDOLPH ROAD
HANSCOM AFB, MA 01731-3010

THORNE LAY
UNIVERSITY OF CALIFORNIA, SANTA CRUZ
EARTH SCIENCES DEPARTMENT
EARTH & MARINE SCIENCE BUILDING
SANTA CRUZ, CA 95064

DONALD A. LINGER
DNA
6801 TELEGRAPH ROAD
ALEXANDRIA, VA 22310

KEITH MCLAUGHLIN
MAXWELL TECHNOLOGIES
P.O. BOX 23558
SAN DIEGO, CA 92123

BRIAN MITCHELL
DEPARTMENT OF EARTH & ATMOSPHERIC SCIENCES
ST. LOUIS UNIVERSITY
3507 LACLEDE AVENUE
ST. LOUIS, MO 63103

JOHN MURPHY
MAXWELL TECHNOLOGIES
11800 SUNRISE VALLEY DRIVE SUITE 1212
RESTON, VA 22091

JAMES NI
NEW MEXICO STATE UNIVERSITY
DEPARTMENT OF PHYSICS
LAS CRUCES, NM 88003

CHARLES ODDENINO
BUREAU OF MINES
810 7TH ST. NW
WASHINGTON, DC 20241

JOHN ORCUTT
INSTITUTE OF GEOPHYSICS AND PLANETARY PHYSICS
UNIVERSITY OF CALIFORNIA, SAN DIEGO
LA JOLLA, CA 92093

FRANK PILOTTE
HQ/AFTAC/TT
1030 S. HIGHWAY A1A
PATRICK AFB, FL 32925-3002

KEITH PRIESTLEY
DEPARTMENT OF EARTH SCIENCES
UNIVERSITY OF CAMBRIDGE
MADINGLEY RISE, MADINGLEY ROAD
CAMBRIDGE, CB3 0EZ UK

JAY PULLI
RADIX SYSTEMS, INC.
6 TAFT COURT
ROCKVILLE, MD 20850

PACIFIC NORTHWEST NATIONAL LABORATORY
ATTN: TECHNICAL STAFF (PLS ROUTE)
PO BOX 999, MS K5-72
RICHLAND, WA 99352

PAUL RICHARDS
COLUMBIA UNIVERSITY
LAMONT-DOHERTY EARTH OBSERVATORY
PALISADES, NY 10964

DAVID RUSSELL
HQ AFTAC/TTR
1030 SOUTH HIGHWAY A1A
PATRICK AFB, FL 32925-3002

PACIFIC NORTHWEST NATIONAL LABORATORY
ATTN: TECHNICAL STAFF (PLS ROUTE)
PO BOX 999, MS K6-84
RICHLAND, WA 99352

LAWRENCE LIVERMORE NATIONAL LABORATORY
ATTN: TECHNICAL STAFF (PLS ROUTE)
PO BOX 808, MS L-202
LIVERMORE, CA 94551

CHANDAN SAIKIA
WOODWARD-CLYDE FEDERAL SERVICES
566 EL DORADO ST., SUITE 100
PASADENA, CA 91101-2560

THOMAS SERENO JR.
SCIENCE APPLICATIONS INTERNATIONAL
CORPORATION
10260 CAMPUS POINT DRIVE
SAN DIEGO, CA 92121

AVI SHAPIRA
SEISMOLOGY DIVISION
THE INSTITUTE FOR PETROLEUM RESEARCH AND
GEOPHYSICS
P.O.B. 2286, NOLON 58122 ISRAEL

ROBERT SHUMWAY
410 MRAK HALL
DIVISION OF STATISTICS
UNIVERSITY OF CALIFORNIA
DAVIS, CA 95616-8671

MATTHEW SIBOL
ENSCO, INC.
445 PINEDA COURT
MELBOURNE, FL 32940

SANDIA NATIONAL LABORATORY
ATTN: TECHNICAL STAFF (PLS ROUTE)
DEPT. 5704
MS 0979, PO BOX 5800
ALBUQUERQUE, NM 87185-0979

LOS ALAMOS NATIONAL LABORATORY
ATTN: TECHNICAL STAFF (PLS ROUTE)
PO BOX 1663, MS D460
LOS ALAMOS, NM 87545

DAVID SIMPSON
IRIS
1616 N. FORT MEYER DRIVE
SUITE 1050
ARLINGTON, VA 22209

LAWRENCE LIVERMORE NATIONAL LABORATORY
ATTN: TECHNICAL STAFF (PLS ROUTE)
PO BOX 808, MS L-195
LIVERMORE, CA 94551

JEFFRY STEVENS
MAXWELL TECHNOLOGIES
P.O. BOX 23558
SAN DIEGO, CA 92123

LOS ALAMOS NATIONAL LABORATORY
ATTN: TECHNICAL STAFF (PLS ROUTE)
PO BOX 1663, MS C335
LOS ALAMOS, NM 87545

BRIAN SULLIVAN
BOSTON COLLEGE
INSITUTE FOR SPACE RESEARCH
140 COMMONWEALTH AVENUE
CHESTNUT HILL, MA 02167

DAVID THOMAS
ISEE
29100 AURORA ROAD
CLEVELAND, OH 44139

NAFI TOKSOZ
EARTH RESOURCES LABORATORY, M.I.T.
42 CARLTON STREET, E34-440
CAMBRIDGE, MA 02142

LAWRENCE TURNBULL
ACIS
DCI/ACIS
WASHINGTON, DC 20505

FRANK VERNON
UNIVERSITY OF CALIFORNIA, SAN DIEGO
SCRIPPS INSTITUTION OF OCEANOGRAPHY IGPP, 0225
9500 GILMAN DRIVE
LA JOLLA, CA 92093-0225

GREG VAN DER VINK
IRIS
1616 N. FORT MEYER DRIVE
SUITE 1050
ARLINGTON, VA 22209

TERRY WALLACE
UNIVERSITY OF ARIZONA
DEPARTMENT OF GEOSCIENCES
BUILDING #77
TUCSON, AZ 85721

LAWRENCE LIVERMORE NATIONAL LABORATORY
ATTN: TECHNICAL STAFF (PLS ROUTE)
PO BOX 808, MS L-205
LIVERMORE, CA 94551

DANIEL WEILL
NSF
EAR-785
4201 WILSON BLVD., ROOM 785
ARLINGTON, VA 22230

JAMES WHITCOMB
NSF
NSF/ISC OPERATIONS/EAR-785
4201 WILSON BLVD., ROOM 785
ARLINGTON, VA 22230

RU SHAN WU
UNIVERSITY OF CALIFORNIA SANTA CRUZ
EARTH SCIENCES DEPT.
1156 HIGH STREET
SANTA CRUZ, CA 95064

JIAKANG XIE
COLUMBIA UNIVERSITY
LAMONT DOHERTY EARTH OBSERVATORY
ROUTE 9W
PALISADES, NY 10964

PACIFIC NORTHWEST NATIONAL LABORATORY
ATTN: TECHNICAL STAFF (PLS ROUTE)
PO BOX 999, MS K5-12
RICHLAND, WA 99352

SANDIA NATIONAL LABORATORY
ATTN: TECHNICAL STAFF (PLS ROUTE)
DEPT. 6116
MS 0750, PO BOX 5800
ALBUQUERQUE, NM 87185-0750

JAMES E. ZOLLWEG
BOISE STATE UNIVERSITY
GEOSCIENCES DEPT.
1910 UNIVERSITY DRIVE
BOISE, ID 83725

OFFICE OF THE SECRETARY OF DEFENSE
DDR&E
WASHINGTON, DC 20330

DEFENSE TECHNICAL INFORMATION CENTER
8725 JOHN J. KINGMAN ROAD
FT BELVOIR, VA 22060-6218 (2 COPIES)

TACTEC
BATTELLE MEMORIAL INSTITUTE
505 KING AVENUE
COLUMBUS, OH 43201 (FINAL REPORT)

PHILLIPS LABORATORY
ATTN: XPG
29 RANDOLPH ROAD
HANSCOM AFB, MA 01731-3010

PHILLIPS LABORATORY
ATTN: GPE
29 RANDOLPH ROAD
HANSCOM AFB, MA 01731-3010

PHILLIPS LABORATORY
ATTN: TSML
5 WRIGHT STREET
HANSCOM AFB, MA 01731-3004

PHILLIPS LABORATORY
ATTN: PL/SUL
3550 ABERDEEN AVE SE
KIRTLAND, NM 87117-5776 (2 COPIES)